INFORMATION TO USERS

This reproduction was made from a copy of a document sent to us for microfilming. While the most advanced technology has been used to photograph and reproduce this document, the quality of the reproduction is heavily dependent upon the quality of the material submitted.

The following explanation of techniques is provided to help clarify markings or notations which may appear on this reproduction.

1. The sign or "target" for pages apparently lacking from the document photographed is "Missing Page(s)". If it was possible to obtain the missing page(s) or section, they are spliced into the film along with adjacent pages. This may have necessitated cutting through an image and duplicating adjacent pages to assure complete continuity.

2. When an image on the film is obliterated with a round black mark, it is an indication of either blurred copy because of movement during exposure, duplicate copy, or copyrighted materials that should not have been filmed. For blurred pages, a good image of the page can be found in the adjacent frame. If copyrighted materials were deleted, a target note will appear listing the pages in the adjacent frame.

3. When a map, drawing or chart, etc., is part of the material being photographed, a definite method of "sectioning" the material has been followed. It is customary to begin filming at the upper left hand corner of a large sheet and to continue from left to right in equal sections with small overlaps. If necessary, sectioning is continued again—beginning below the first row and continuing on until complete.

4. For illustrations that cannot be satisfactorily reproduced by xerographic means, photographic prints can be purchased at additional cost and inserted into your xerographic copy. These prints are available upon request from the Dissertations Customer Services Department.

5. Some pages in any document may have indistinct print. In all cases the best available copy has been filmed.

University Microfilms International
300 N. Zeeb Road
Ann Arbor, MI 48106

Putman, Clive Andrew

SYNCHRONIZATION OF FREQUENCY HOPPED SPREAD SPECTRUM SYSTEMS

City University of New York PH.D. 1983

SYNCHRONIZATION OF FREQUENCY HOPPED SPREAD SPECTRUM SYSTEMS

by

CLIVE A. PUTMAN

A dissertation submitted to the Graduate Faculty of Electrical Engineering in partial fulfillment of the requirements for the degree of Doctor of Philosophy, The City University of New York.

1983

This manuscript has been read and accepted for the Graduate Faculty in Engineering in satisfaction of the dissertation requirement for the degree of Doctor of Philosophy.

26/5/83
date

Chairman of Examining Committee

26/5/83
date

Executive Officer

Supervisory Committee

City University of New York

Abstract

SYNCHRONIZATION OF FREQUENCY HOPPED SPREAD SPECTRUM SYSTEMS

by

CLIVE A. PUTMAN

Adviser: Professor Donald Schilling

The frequency hopped spread spectrum waveform is commonly used by communications systems for its ability to combat intentional jamming and its inherent diversity. It can therefore be expected that these systems will be required to operate in jamming and fading environments. Since synchronization is a vital aspect of spread spectrum communications, it is important to predict synchronization performance in such adverse environments.

Several schemes for the acquisition and tracking of frequency hopped signals are discussed. Formulas for describing system performance in terms of detection reliability, acquisition time and mean time to loss of lock are presented. Mathematical models characterizing the interference and multipath fading channel are developed. The performance of some example systems, with application to particular environments, is then analysed and results computed.

I N D E X

Page

LIST OF FIGURES

1. INTRODUCTION

1.1 FREQUENCY HOP AS A SPREAD SPECTRUM WAVEFORM

Original work by Shannon in the field of statistical communications showed that the capacity of a channel to transfer error-free information is enhanced with increased bandwidth. This is the basis for spread spectrum techniques. A spread spectrum system is a system that produces a signal with a bandwidth much wider than the information bandwidth. Through the properties of pseudorandom code modulation these systems can provide resistance to interference and multipath fading, low detectability, multiple access and other useful capabilities.

The more common modulation formats include direct sequence (DS), in which a carrier is phase modulated by a digital code sequence having a bit rate much higher than the information signal bandwidth, and frequency hopping (FH), in which the carrier is frequency shifted in discrete increments in a pattern determined by a digital code sequence. For short, intermittently established mobile links, DS suffers from the 'near-far' problem associated with other channel users located close to the receiver causing a severe reduction in processing gain. The FH waveform is less severely affected in this situation and, coupled with its inherent diversity and ease of implementation, is more likely to be used.

1.2 SYNCHRONIZATION REQUIREMENTS

A generalized FH spread spectrum system [1]-[3] is illustrated in Fig. 1.1. A central feature is the pseudorandom code generators at both transmitter and receiver, capable of producing identical codes with proper synchronization. The pseudorandom code sequence is used to switch the carrier frequency via a frequency synthesizer and wideband mixer. When the synthesizer in the receiver is switched with the synchronized sequence the frequency hops on the received signal will be removed, leaving the original unmodulated signal. The requirement for accurate synchronization is thus of major importance in the analysis and design of FH spread spectrum systems.

Synchronization is typically established through the following processes: coarse synch, or acquisition, which aligns the receivers local code to within half a code bit (chip) of the received code, followed by fine synch, or tracking, which reduces the alignment error to as small a value as possible and maintains it that way. For long codes it is generally not feasible to search the whole code for the correct code phase and some apriori information about the code phase must be provided by other means such as a known code preamble or time of day synchronism. A tactical communications environment obviously implies rapid and reliable acquisition and accurate tracking of the FH waveform.

1.3 ENVIRONMENTAL CONSIDERATIONS

Several schemes for the acquisition and tracking of spread spectrum signals in additive white Gaussian noise have been well described in the literature [3]-[5]. The intention here is to develop analytical models and mathematical formulas which characterize the performance of these schemes in adverse environments.

A typical scenario for a mobile tactical communications receiver is depicted in Fig. 1.2. Propagation is likely to occur through fading media. The channel is physically characterised as having a dominant signal path in addition to a large number of independent multipaths. Generally, this model typifies observed behavior for fast fading channel variations, although in addition there may be long term slow variations. The result is a random amplitude and phase change at the receiver. Severe multipath results in distortion of the received hop waveform.

Unwanted signals due to intentional jamming by enemy transmitters and unintentional jamming due to other friendly users in a multiple access environment will be picked up at the receiver. Assuming these signals are unsynchronized, they will be removed most of the time by the IF filter in the receiver, but there is a certain finite probability that interception will occur and degrade receiver performance.

2. GENERAL ANALYSIS

2.1 SIGNAL CORRELATION

The acquisition and tracking processes will normally involve some type of correlation of the received FH waveform with a locally generated signal. The essential elements are shown in the block diagram of Fig. 2.1a. The received signal is first multiplied by the locally generated signal and then filtered by an IF bandpass filter. The output waveform during the i^{th} hop interval can be characterized as

$$S_o(t) = a_i \cos(\omega_o t + \theta_i) + g_i(t) \qquad (2.1)$$

where $g_i(t)$ is a Gaussian process with zero mean and variance σ^2, and ω_o is the IF midband frequency. In the case of the benign environment, $g_i(t)$ is a noise process. This signal can also be written as

$$S_o(t) = r_i(t) \cos[\omega_o t + \theta_i + \phi_i(t)] \qquad (2.2)$$

where $r_i(t)$ is a Rician distributed process. The signal is applied to an envelope detector which rejects the carrier frequency but passes the modulation envelope. The output voltage during i^{th} hop, $r_i(t)$, has a Rice probability density function given by

$$p_{s,n}(r) = \frac{r}{\sigma^2} e^{-(r^2+a_i^2)/2\sigma^2} I_o(ra_i/\sigma) \qquad (2.3)$$

where I_0 is the modified Bessel function of the first kind, order zero. When there is no correlation between the received and locally generated signal a_i is zero, $g_i(t)$ is a noise process, and the probability density function of $r_i(t)$ becomes the Rayleigh distribution function,

$$p_n(r) = \frac{r}{\sigma^2} e^{-r^2/2\sigma^2} . \tag{2.4}$$

Consider correlation over a period of M hops, resulting in M pulses with amplitudes r_1, r_2, r_3, ... r_M available from the receiver. The problem consists of determining whether or not these M pulses are due to signal-plus-noise or whether they are due to noise alone. It is assumed that envelopes of distinct received hops are statistically independent. The probability density function for the envelope of M pulses of noise only is then

$$p_n(M,r) = \prod_{i=1}^{M} p_n(r_i), \tag{2.5}$$

and the probability density function for the envelope of M pulses of signal-plus-noise is

$$p_{s,n}(M,r) = \prod_{i=1}^{M} p_{s,n}(r_i). \tag{2.6}$$

The detection process is equivalent to determining which of the two density functions (2.5) or (2.6) more closely describes the output of the receiver.

2.2 LINEAR INTEGRATION DETECTION

For analytical convenience we consider the use of a square-law detector combined with an integrator as shown in Fig. 2.1b. As shown in Appendix A, by forming the sum of squares of Rician variates this arrangement comprises the optimum detector for low signal-to-noise ratios and is approximately optimum for high signal-to-noise ratios. Thus the output of the integrator is

$$z = \sum_{i=0}^{M} r_i^2(t) \tag{2.7}$$

For convenience we define a normalized variable Z such that

$$Z = z/\sigma^2 \tag{2.8}$$

It can be shown [6] that the probability density function of Z is the chi-squared function,

$$p_Z(x) = \tfrac{1}{2}(x/S)^{(M-1)/2} e^{-(x+S)/2} I_{M-1}(\sqrt{xS}) \tag{2.9}$$

where we define

$$S = \sum_{i=0}^{M} a_i^2/\sigma^2,$$

and I_{M-1} is the modified Bessel function of the first kind, order M-1.

At the end of the integration period MT_H, where T_H is

the hop period, the output z is compared to a threshold level v. The probability that z exceeds the threshold is the probability of a 'hit' given by

$$P_h = P\{z>v\} = \int_V^\infty p_Z(x)dx, \tag{2.10}$$

where V is the normalized threshold, $V = v/\sigma^2$. This can be expressed in terms of the generalized Marcum Q function [7] as,

$$P_h = Q_M(\sqrt{S},\sqrt{V}) \tag{2.11}$$

where $Q_M(u,w) = \int_w^\infty x(x/u)^{M-1}e^{-(u^2+x^2)/2}I_{M-1}(ux)dx$.

Defining the average energy per hop in the IF waveform for the case of the benign environment as

$$E_H = (T_H/M).\sum_{i=1}^{M} a_i^2/2 , \tag{2.12}$$

and the noise power as $\sigma^2 = N_o/T_H$ where $1/T_H$ is the IF equivalent noise bandwidth and N_o is the one sided noise power spectral density, then

$$S = 2ME_H/N_o \tag{2.13}$$

is seen to be indicative of the signal strength.

Now we are interested in two error conditions which can

occur. Firstly, there is the probability of a false hit due to interference and noise causing a threshold exceedence. This is obtained from (2.11) as

$$P_{fh} = Q_M(\sqrt{S_I}, \sqrt{V}) \tag{2.14}$$

where S_I is the signal strength due to received interference waveforms (in the case of the benign environment this is zero). Secondly there is the probability that the threshold is not exceeded when in fact the desired signal with the correct code phase is present at the receiver input. This is the probability of no hit given by the complement of (2.11) expressed as

$$P_{nh} = 1 - P_h = Q_M{}^c(\sqrt{S_T}, \sqrt{V}) \tag{2.15}$$

where S_T is the signal strength due to desired and unwanted signal waveforms, and in which the notation $Q_M{}^c$ is used to denote the complementary Q_M function.

2.3 BINARY INTEGRATION DETECTION

The problem with a detector which integrates linearly over several hop intervals is that during the process interfering signals may be received on a relatively small number of hops yet are sufficiently strong to cause a false

hit condition. A method of detection which reduces this problem is shown in Fig. 2.1c. Basically it uses the criterion that correlation must occur for L out of N hop intervals, a form of binary integration [8]. At the end of each hop interval the output of the integrator is compared to the first threshold V and the result stored digitally. After N such comparisons the results are summed digitally and if the sum exceeds the second quantized threshold L, a hit is declared.

The probability of j threshold exceedances in N comparisons is the binomial distributed function,

$$b(j,N,P_h) = \binom{N}{j} P_h^{\,j} (1-P_h)^{N-j} \quad , \tag{2.16}$$

where P_h is given by (2.11) with a value of unity for M. Since the overall probability of a hit is the probability of L or more threshold exceedances, the probability of detection for this system is

$$P_H = \sum_{j=L}^{N} \binom{N}{j} P_h^{\,j} (1-P_h)^{N-j} \quad . \tag{2.17}$$

Similary the overall probability of no hit is the probability of less than L threshold exceedances, or

$$P_{NH} = \sum_{j=0}^{L-1} \binom{N}{j} (1-P_{nh})^{j} P_{nh}^{\,N-j} \quad , \tag{2.18}$$

and the overall probability of a false hit is

$$P_{FH} = P_H|_{S=S_I} \quad . \tag{2.19}$$

An obvious extension to the above scheme is to relax the requirement that M is unity and integrate over M hops before comparing the integrator output to the first threshold.

Thus the advantage of the binary integrator is that it is less sensitive to the effects of a single large interference pulse caused by correlation with a jammed frequency slot. In the usual integrator, the full energy of the interference pulse is added. In the binary integrator detector, however, it contributes no more that would any other pulse that crosses the first threshold since a quantized level is recorded for that slot no matter what the amplitude.

Equations (2.18) and (2.19) are then general in the sense that they yield the probabilities of no hit and a false hit after a correlation dwell time of NM hops, with N=1 for the case of pure linear integration, and M=1 for the case of pure binary integration. Inherent in each of the equations are two thresholds, V and L.

2.4 SEARCH/LOCK STRATEGY

The search/lock (S/L) strategy is a logical procedure by which the operation of the synchronizer is controlled.

Information received from the threshold detector, that is whether or not the threshold is exceeded after signal correlation, is interpreted by a control system which decides whether or not a signal of the correct code phase is present at the receiver input and takes the appropriate action. Selection of the S/L strategy will have an important effect on the time required to test a phase position (cell), and thus on the time required to achieve synchronization and the time for which synchronization is likely to be maintained.

One type of strategy is shown in state transition form in Fig. 2.2a. The first state represents the initial test of the cell during the search process. A hit at the end of the test results in a transition to the next state, otherwise the cell is rejected, resulting in a phase step to the next cell. A further test in the second state results in either a transition back to state one or on to the next state, and so on. A hit in state m results in a transition to the lock mode, whereupon continued hits will maintain control in the lock state, otherwise control is transfered to the alternative lock states as during the search phase. A miss in state n results in rejection of the cell and a return to the search phase with the next cell. This S/L strategy is analogous to a counter with n possible counts and is referred to as an 'up-down counter' strategy.

Another type of S/L strategy is the 'consecutive count' strategy of Fig. 2.2b. In this case a miss at any time

during the search phase causes immediate rejection of the cell, and a hit at any time during the lock phase causes immediate return of control to the first lock state.

A convenient analytical approach is to describe the S/L strategy as a finite Markov chain with absorbing boundaries [9]. The Markov chain representations for the 'up-down' and 'consecutive count' strategies are shown in Figs. 2.3a,b respectively. In each case there are two absorbing states, i.e. states from which there is no exit, representing rejection of the current cell. The diagrams are characterized by states connected by directed lines that indicate the probability of going from the originating state to the terminating state. We define p_s and q_s as the probability of a hit and no hit respectively, given that control is in the search mode. These probabilities are held distinct from p_l and q_l, the probability of a hit or no hit in the lock phase, since it is likely that detector parameters will differ for the two phases. It is assumed that these probabilities are constants. The times required to make transitions are times taken to perform the correlation tests. Once again we differentiate between the search and lock phases and define the test times as τ_s and τ_l respectively.

A Markov chain can be described by its transition matrix P whose element p_{ij} is the probability of transition from state i to state j, and its state at any initial time. If $\underline{x}_i$ is the vector probability whose element x_{ij} is the

probability of being in state j at the i^{th} step, then

$$\mathbf{x}_{i+1} = \mathbf{P}\mathbf{x}_i \ . \tag{2.20}$$

Now when the Markov chain possesses absorbing states, P can be rearranged so that

$$\mathbf{P} = \begin{bmatrix} \mathbf{I} & \mathbf{\emptyset} \\ \mathbf{R} & \mathbf{Q} \end{bmatrix} \tag{2.21}$$

where I is an identity matrix relating to all absorbing states, $\emptyset$ is a matrix of all zeros, Q is a submatrix containing the transition probabilities of the transient states, and R is a submatrix containing transition probabilities from transient to absorbing states.

Given that the process begins in state i, it may be absorbed in state j in one or more steps. For a single step the probability of absorbtion is p_{ij}. If the process is not absorbed, it can move to either another absorbing state (and cannot reach state j) or to a transient state k. In the latter case the probability of being absorbed in state j is b_{jk} for any transient state k. If T is the set of all transient states we can write

$$b_{ij} = p_{ij} + \sum_{k \in T} p_{ik} b_{kj} \ ,$$

which in matrix form is

$$B = R + QB = NR \tag{2.22}$$

where $N = (I - Q)^{-1}$ is known as the fundamental matrix. For S/L strategy Markov chains b_{n1} is the probability of entering the lock mode P_L.

Let n_j be the total number of times that the process is in state j where j is a transient state. The total time t that a process is in transient states is then

$$t = \sum_{j \in T} n_j \ . \tag{2.23}$$

Now it can be shown [10] that the matrix $[E_i\{n_j\}]$ composed of elements formed by the mean number of total times the process is in state j starting in state i is

$$[E_i\{n_j\}] = N \ , \quad i,j \in T \tag{2.24}$$

Hence the mean time the process is in a transient state starting in state i is the n-component vector

$$\underline{T} = [E_i\{t\}] = N \underline{\tau} \ , \tag{2.25}$$

where $\underline{\tau}$ is an n-component column vector whose components are the respective cell test times for each state. This equation allows us to find the mean time taken to test a cell, or the mean dwell time, from the first element of $\underline{T}$.

$$T_D = t_1 \ . \tag{2.26}$$

and the mean time spent in the lock mode, from

$$T_L = t_{m+1} \ . \tag{2.27}$$

An alternative analytical technique which does not require matrix computations involves transformation of the state transition diagrams into signal flow graphs [11]. The 'up-down' and 'consecutive count' strategies of Figs. 2.2a,b can then be represented by the signal flow graphs of Figs. 2.4a,b respectively. The variable z represents a delay of one unit time, in this case the detector integration times, and we assume that,

$$\tau_1 = \mu\tau_s \ . \tag{2.28}$$

Discrete linear system analysis can now be applied.

Defining $p_{ij}(n)$ as the time invariant probability of going from state i to state j in n steps, we may obtain the generating function $P_{ij}(z)$ as the Z-transform of $p_{ij}(n)$,

$$P_{ij}(z) = \sum_{n=0}^{\infty} z^n p_{ij}(n). \tag{2.29}$$

The generating function is identically the graph transfer function and can be obtained using signal flow graph

reduction techniques [12]. The probability of going from state i to j is then

$$P_{ij} = \sum_{n=0}^{\infty} p_{ij}(n) = P_{ij}(1) \quad . \tag{2.30}$$

The mean time to achieve this transition is

$$\bar{T}_{ij} = \sum_{n=0}^{\infty} np_{ij}(n) = \frac{d}{dz} P_{ij}(1) \quad . \tag{2.31}$$

The probability of entering the lock mode for the system can then be obtained from

$$P_L = P_{1,m+1}(1) \quad . \tag{2.32}$$

and $\bar{T}_{1,n+1}$ yields the mean dwell time normalized to the detector integration time, so that

$$T_D = \tau_s \frac{d}{dz} P_{1,n+1}(1) \quad . \tag{2.33}$$

Similarly the mean in-lock time is given by

$$T_L = \tau_1 \frac{d}{dz} P_{m+1,n+1}(1) \quad . \tag{2.34}$$

The above analysis techniques provide a unified approach to the S/L strategy problem. It may however be desired to investigate the search process or the tracking process separately. In the case of the latter there is no

problem - the search states are simply deleted. In the case of the search process, entrance into the lock mode must be considered. For Markov chain analysis the entire lock mode is represented by a single transition with unit probability, Fig.2.5a, since, given enough time, a system will always lose lock. The signal flow graph analysis equivalent is shown in Fig.2.5b, where k is the number of unit time intervals spent in the lock state.

In general it was found that the Markov chain analysis is more elegant for a unified approach, whereas the signal flow graph technique is more convenient for analysing the acquisition and tracking phases separately.

2.5 PERFORMANCE CRITERION

In order to measure and compare the performance of various acquisition and tracking systems we need to choose some criterion. The choice will essentialy depend on the application.

With regard to the search mode we are interested in the probability of detecting a wanted signal of the correct code phase when present at the receiver input. This is the detection probability P_D. Since we would expect this quantity to be close to unity we choose as our performance parameter its complement, the miss probability P_M.

$$P_M = 1 - P_D \quad . \tag{2.35}$$

Since these quantities depend on the detector threshold setting, they are only defined for a given probability that a signal of the correct code phase was deemed present at the receiver input when in fact it was not, i.e. the false alarm probability P_{FA}. The detection probability is given by P_L with $S = S_T$ and P_{FA} is given by P_L with $S = S_I$.

Another quantity we are interested in for search mode performance evaluation is acquisition time. Given the mean dwell time T_D, acquisition time is clearly determined by the number of cells, N_S, to be tested in each search of the uncertainty region. The mean search time is then,

$$T_S = N_S T_D \quad . \tag{2.36}$$

It should be observed that T_D is computed using transition probabilities equal to the false hit probability in the search mode.

The miss probability and the mean search time are meaningful performance parameters for systems which are required to reliably detect the first occurence of the correct code epoch during a single search of the uncertainty region. Such a system might, for example, rely on a fixed code preamble to define a synch prefix.

If we consider a system which can tolerate one or more code epoch detection misses and yet continue to seek

acquisition it is of interest to characterize acquisition time distribution in terms of P_D and P_M as follows: Let us assume that the mean search time T_S is a constant for each uncertainty region search. We can then sketch the distribution and density functions of the acquisition time T_{acq} as in Figs.2.6a,b respectively. The mean and variance of this random variable can then be found as outlined in Appendix B.

A more informative statistical measure of acquisition time is that time within which acquisition is achieved 90 percent of all attempts. This we shall call the 90^{th} percentile acquisition time, T_{90}. Define ξ as integer part of t/T_S. Then from Fig. 2.6b

$$P[T_{acq}<t] = \sum_{n=0}^{\xi-1} P_D P_M^n + (t/T_S-\xi)P_D P_M^{\xi}$$

$$= 1 - P_M^{\xi}[1-(t/T_S-\xi)P_D] \quad . \qquad (2.37)$$

Hence for 90^{th} percentile acquisition

$$1 - P_M^{\xi}[1-(T_{90}/T_S-\xi)P_D] = 0.9$$

so that

$$T_{90} = T_S[(1-0.1/P_M^{\xi})/P_D + \xi] \quad . \qquad (2.38)$$

Note that this equation does not have a unique solution, and must be solved by incrementing ξ from 0 until $[T_{acq}/T_S-\xi]<1$

is satisfied.

With regard to the tracking mode, there are two possibilities for entering the lock state. Either the correct code epoch may have been detected causing the system to correctly enter the lock mode, or a false alarm may have caused the system to incorrectly enter the lock mode. The requirements for the tracking phase are to maintain tracking of the correct code phase in the former case, yet quickly reject the false lock condition to allow resumed search in the latter case. In-lock performance is therefore characterized by mean time to loss of lock T_{LL} for a given mean time to reject false lock T_{FL}. Detector threshold setting is then encompassed by this definition. It should be observed that T_{LL} is computed using transition probabilities equal to the hit probability in the lock mode, and T_{FL} is computed using transition probabilities equal to the false hit probability in the lock mode.

3. ENVIRONMENTAL MODELLING

3.1 FADING CHANNEL MODEL

We consider a channel in which fading manifests itself as a single scattering from a large number of independent elements or 'scatterers'. These scatterers might be orbital dipoles or differential elements of either the troposphere or the ionosphere.

Let the component received from the j^{th} scatterer during the i^{th} hop be

$$s_{ij}(t) = \beta_{ij} A(t) \cos[\omega_o(t-\tau_{ij})] , \qquad (3.1)$$

where A(t) is a rectangular pulse of duration T_H, amplitude A, and τ_{ij} is the initial propogation delay. Since we seldom know the value of each τ_{ij} precisely, and since small perterbations in the value are important, we express τ_{ij} in the form

$$\tau_{ij} = r_{ij} + \gamma_{ij}/\omega_i , \qquad (3.2)$$

where r_{ij} is the known or gross value of τ_{ij} and γ_{ij} accounts for the perterbations and is a uniformly distributed variable over the interval $(-\pi,\pi)$.

The total received scatter component is obtained by summing over all the scatterers composing the medium. Specifically,

$$s_i(t) = A(t) \sum_j \beta_{ij} \cos[\omega_i(t-r_{ij}) - \gamma_{ij}] \ . \qquad (3.3)$$

It is reasonable to assume that the β_{ij} are independent of the γ_{ij}. Since the number of scatterers is large, the central limit theorem permits us to assume that the scatter component is Gaussian.

These assumptions imply that the mean value of s(t) is zero and that, since the total delay r_{ij} is many wavelengths, the total received signal during the i^{th} hop is described by,

$$S_r(t) = A(t)[\alpha_i \cos(\omega_i t+\theta_i) + \sum_j \beta_{ij} \cos\{\omega_i(t-r_{ij})-\gamma_{ij}\}] + n(t) \qquad (3.4)$$

where n(t) is a Gaussian noise process. In this equation the first term represents a specular component defined as a dominant signal path being assumed to arise from a relatively stable ray path such as a well formed layer reflection or ground wave.

The autocorrelation function of $s_i(t)$ is given by,

$$R_i(t,\tau) = \frac{1}{2} \sum_j \overline{\beta_{ij}^2} A(t-r_{ij})A(t-r_{ij})\cos[\omega_i(t-\tau)] \ . \qquad (3.5)$$

It is convenient to introduce the multipath delay scatter function $\rho(r)$ associated with each delay r_{ij} and frequency ω_i as

$$\rho_i(r) = \sum_j \overline{\beta_{ij}}^2 \tag{3.6}$$

and the channel multipath spread as

$$T_M = [\rho^2(r)]^{-1} \ . \tag{3.7}$$

Since attempts to measure the characteristics of fading dispersive channels yield smooth densities, received waveforms from different scatterers being indistinguishable, we envisage $\rho(r)$ as a smooth density rather than a point function. We can now rewrite equation (3.5) as

$$R_i(t,\tau) = \frac{1}{2}\int \rho_i(r)A(t-r)A(\tau-r)\cos[\omega_i(t-\tau)]dr \ . \tag{3.8}$$

We further specify that,

$$\int \rho_i(r)dr = \text{constant} = b_i. \tag{3.9}$$

The average received scatter power at time t is defined by

$$P(t) = R(t,t) \ , \tag{3.10}$$

so that during the i^{th} hop,

$$P_i(t) = \frac{1}{2}\int \rho_i(r)A^2(t-r)dr \ . \tag{3.11}$$

This is precisely the convolution of $A^2(t)$ and the delay scattering function $\rho(t)$. If $A^2(t)$ is an impulse function the profile of the time distribution of average power $P(t)$ will be proportional to $\rho(t)$. This situation prevails when T_H is much less than T_M, and $A^2(t)$ appears to be impulsive with respect to $\rho(t)$. This suggests a means for measuring the channel scattering function.

In an endeavour to obtain a simple description of the fading channel, let us adopt as an example scattering function the uniform density of Fig.3.1a. Although this results in a gross description of the channel model, the analysis can be applied to any suitable function. Performing the convolution with our pulse amplitude function of Fig.3.1b results in the average power function of Fig.3.1c. Thus the received process is spread over a time duration of T_H+T_M seconds. In fact, this will be approximately correct for most scattering functions [13].

Now the receiver correlates this process with a locally generated waveform, so that the receiver is essentially matched to a waveform of pulse duration T_H. Multipath spread therefore results in a loss of correlation. Specifically, the scatter component energy in the i^{th} hop of the IF waveform is

$$E_i = \int_0^{T_H} P_i(t)dt \ . \qquad (3.12)$$

Applying this to the function of Fig.3.1c results in the

correlation diagram of Fig.3.1d, where τ is the relative delay between the received and locally generated waveforms.

The pertinent question now is, what is the time distribution of the power in the specular component relative to the scatter component? A reasonable and tangible assumption is that peak correlation instants coincide. In the uniform fading case this implies that the specular component receives a relative delay of $T_M/2$ seconds.

We are now in a position to compute the average energy per hop in the IF waveform of equation (3.5). The average energy per hop in the specular component is

$$E_\alpha = (T_H/M) \cdot \sum_{i=1}^{M} A^2 \alpha_i^2/2 = \tilde{a} E_H \ . \qquad (3.13)$$

where $\tilde{a} = (1/M) \sum_{i=1}^{M} \alpha_i^2$,

and the energy per hop in the scatter component is

$$E_\beta = (1/M) \cdot \sum_{i=1}^{M} E_i = \tilde{b} d E_H \ . \qquad (3.14)$$

where $\tilde{b} = (1/M) \sum_{i=1}^{M} b_i$,

and d is a factor which accounts for the average loss in correlation due to multipath spread. Essentially $\tilde{b}$ is summed over all multipaths received during the M hop

integration period. Assuming peak correlation,

$$d = 1 - T_M/4T_H \ , \tag{3.15}$$

where T_M typifies the channel multipath spread for the band over which the M frequencies are distributed. Common values for this quantity over a given frequency band are obtainable from the literature [14].

We recall that the received process is the superposition of the contributions from all the scatterers composing the medium. Therefore it includes components that have been subjected to range delays of approximately $\pm T_M/2$ seconds, and the received process for any scattering function will be spread over approximately T_H+T_M seconds. Thus if T_M is much less than T_H there is no apparent spreading of the received waveform. There are two possible reasons for this. Either T_H is made large, i.e. a slow hop rate, in which case multipath spread is negligible, or T_M is small and in the limit $\rho(r)$ tends to an impulse function $\delta(r)$. In the latter case the channel is the nondispersive Rician flat-fading channel, a situation which is approximated in the former case. However, as T_M approaches T_H the channel becomes time dispersive, often referred to as a frequency selective fading channel. It is under these conditions that the inherent frequency diversity of the frequency hopped waveform finds advantage.

Consider the cross correlation function defined by

$$C(t,\omega_1,\omega_2) = E\{s_1(t),s_2(t)\}$$

$$= \tfrac{1}{2}\int \rho(r)\cos[(\omega_1-\omega_2)(t-r)]dr \ . \qquad (3.16)$$

We enquire about the difference $\omega_1-\omega_2$ for which the cross correlation function vanishes, that is

$$C(t,\omega_1-\omega_2) = 0 \ , \qquad (3.17)$$

thereby specifying the frequency separation B_c beyond which two samples of the received process are independent. For uniform spreading where

$$\omega_1-\omega_2 = 2\pi/T_M \ , \qquad (3.18)$$

we have

$$C(t,\omega_1-\omega_2) = \tfrac{1}{2}\int_0^{T_M} (\tilde{b}/T_M)\cos[2\pi(t-r)/T_M]dr \ . \qquad (3.19)$$

This motivates the definition

$$B_c = 1/T_M \qquad (3.20)$$

as the channel coherence frequency. We now assume that the number of frequency slots available, F, have center frequencies that are uniformly distributed over a band of

width B. Then in order for our model to be valid in the sense that fading is independent from hop to hop, we require that

$$B_c \ll B/F \ , \tag{3.21}$$

a situation which will, with good design, normally prevail.

For comparitive analysis we equate the sum of the energies in the specular and scatter components to a constant, E_H. Hence we take

$$\tilde{a} + \tilde{b} = 1 \ . \tag{3.22}$$

The quantities $\tilde{a}$ and $\tilde{b}$ are indicative of the relative strengths of the specular and scatter components respectively, and are assumed fixed over the acquisition period although they may have long term slow variations.

The variance of $g_i(t)$ is now the sum of the rms power in the noise and scatter processes, or

$$\sigma^2 = N_o/T_H + \tilde{b}dE_H/T_H \tag{3.23}$$

Signal strength can then be calculated as

$$S_F = 2ME_H\tilde{a}/(N_o+\tilde{b}dE_H) \ . \tag{3.24}$$

This is the fading channel model, equation (3.24)

permitting us to predict detection reliability in such environments. It should be noted that although the scatter component has been modelled as a Gaussian process, it is not being treated as noise. This can be seen by noting that the detection threshold is normalized to $V=v/(N_o/T_H)$ for noise only conditions, but must be re-normalized to

$$V'=V/(1+\tilde{b}dE_H/N_o) \qquad (3.25)$$

when signal is present.

3.2 THE INTERFERENCE MODEL

We now consider the effect of interference generated by other users and intentional jamming. In the situation where other unsynchronized users in the band are hopping over the same set of frequencies there is a finite probability that during an attempt to synchronize to the desired signal, a signal from one or more of the other transmitters will be received, thereby increasing the false alarm probability. If there is one other user active the probability of reception during a given hop is simply 1/F. If there are I other users active the probability that no interfering signal is received during a given hop is

$$\eta = (1-1/F)^N . \qquad (3.26)$$

In a tactical environment the major threat to communications is intentional jamming. Faced with frequency hopping evasion, the jammer would be forced to jam a random selection of frequencies. If a single transmitter hopped randomly over the F frequency slots is used, the threat is limited to that of another user, although the received energy may well be greater. If several, say I, transmitters are used continuously, known as comb jamming, equation (3.26) is approximately valid when F is large. We therefore henceforth refer to other users and jammers collectively as interferers, the magnitude of the threat being determined by the interfering signal strength.

Equation (3.26) can be written in terms of the fraction of the hop set occupied,

$$G = I/F \ , \tag{3.27}$$

as

$$\eta \approx 1 - G + G^2/2! - G^3/3! \cdots \tag{3.28}$$

The probability that at least one other interfering signal is received during a given hop is then

$$\rho = 1-\eta \ . \tag{3.29}$$

If we integrate linearly over M hops, the probability that at least one interfering signal is received on j slots is

$$b(j,M,\rho) = \binom{M}{j}\rho^{j}\eta^{M-j} \quad . \tag{3.30}$$

The probability of a false hit is then determined by multiplying the probability of j slots being jammed and summing over j,

$$P_{fh} = \sum_{j=0}^{M} b(j,M,\rho)Q_{M}(\sqrt{S_I},\sqrt{V}) \tag{3.31}$$

with $S_I = 2jJE_H/N_o$, where J is the average interfering signal power to desired signal power ratio per slot occupied.

We now assume that where an interferering signal and the desired signal are present in the same slot their powers are additive. This is not unreasonable since the phases of the wanted and unwanted signals are expected to be random and independent. We can then write that the probability of no hit is given by

$$P_{nh} = \sum_{j=0}^{M} b(j,M,\rho)Q_{M}^{c}(\sqrt{S_T},\sqrt{V}) \tag{3.32}$$

with

$$S_T = 2(jJ + M)E_H/N_o \quad .$$

3.3 THE COMBINED MODEL

To quantify performance for a fading environment with interferers present it is analytically convenient to assume that the power of the interfering signals lie in the specular components. The probability of no hit is then

$$P_{nh} = \sum_{j=0}^{M} b(j,M,\rho) Q_M^{\,c}(\sqrt{S_T},\sqrt{V'}) \qquad (3.34)$$

with

$$S_T = 2(jJ+M\tilde{a})E_H/[N_o+\tilde{b}dE_H] \ .$$

4. SYNCHRONIZATION TECHNIQUES

4.1 MATCHED FILTER ACQUISITION

A matched filter is a passive correlator intended to recognize a particular M hop sequence in an FH waveform. As shown in the block diagram of Fig. 4.1a, the selectively delayed outputs of M parallel correlators and detectors are summed and compared to a threshold. The M hop sequence establishes a code epoch and the filter searches the incoming hop sequence for this prefix. The structure as shown provides near optimal detection as the prefix is received. Synchronization is declared when the threshold is exceeded.

The prefix must be chosen from the particular sequence of frequencies which is expected to arrive during the interval that the search takes place, and this interval must be sufficiently long so as to accommodate the entire uncertainty region. By changing the M local oscillator frequencies, the synch prefix is varied.

Since the matched filter arrangement of Fig. 4.1a forms the sum of squares of M Rician variates, the analysis of the previous sections applies and a statistical measure of the reliability of the synchronization indication is provided by equations (2.14) and (2.15). Also since the search process takes place in real time, $\tau_s = T_H$, the number of cells to be searched N_S is just the number of hops in the uncertainty region N_U plus the number of delays, i.e.,

$$N_S = N_U + M \ . \qquad (4.1)$$

A matched filter utilizing quantized integration is shown in Fig. 4.1b. As discussed in section 2.3 this arrangement prevents the system from being overwhelmed by a few strong narrowband interfering signals. Equations (2.17) and (2.18) now apply.

4.2 SERIAL SEARCH ACQUISITION

Serial search involves active correlation of the received FH waveform with a similar locally generated FH waveform, as shown in Fig. 4.2a. At the end of the integration period the correlator output is compared to a threshold, and if the threshold is exceeded a hit is declared. Depending on the control strategy, one or more hits may be required before synchronization is declared. If the threshold is not exceeded after the first or, again depending on the control strategy, later integration periods, the cell is rejected and the search continued. Searching of the received FH waveform for the correct code phase is achieved by adjusting the phase of the receiver clock and correlating again. The serial search scheme implemented with binary integration is shown in Fig. 4.2b. Thus the cell test time is the integration time MNT_H.

In general there are two possible methods for adjusting the local code phase: Either the receivers code generator clock is inhibited for a fraction of a period thereby retarding the local code phase, or the clock is advanced for a fraction of a period thereby advancing the local code phase. The diagram of Fig. 4.3 demonstrates, with the aid of a simple example, the relative differences in the resulting search rates. Receiver waveforms (a) and (b) are the result of inhibiting the local waveform generator for up to one transmitter hop period after each cell rejection (M=N=1 here), called 'stepped serial search'. In both cases the receiver code must be advanced to the end of the uncertainty region (here 3 hops). Receiver waveforms (c) and (d) are the result of a 'fast hop' search in which the receiver code must be retarded to the beginning of the uncertainty region, and the receiver hop period subsequent to cell rejection is less than the transmitter hop period. In all examples the worst case initial phase alignment is shown. Waveform (a) corresponds to slipping the receiver code half a bit after every cell rejection and is seen to be the slowest search method. Waveform (d) corresponds to a receiver hop rate twice that of the transmitter and is seen to be the fastest.

We define the receiver to transmitter hop period ratio as

$$\delta = [T_H+\Delta]/T_H \qquad (4.2)$$

where Δ is either a positive time delay increment for stepped search or a negative time delay decrement for fast hop search. It is easily shown that the search rate for either search method is $\delta/|\delta-1|$ so that for serial search,

$$N_s = N_u \delta/|\delta-1| \ . \tag{4.3}$$

Increasing the search rate to speed up acquisition time is not without its compromise - the average energy detected is less. It is found, Appendix C, that the average desired signal energy must multiplied by the factor,

$$d_s \approx (5-\delta)/4 \ , \quad \delta>1 \tag{C1}$$

$$d_s = \delta \ , \quad \delta<1 \tag{C2}$$

in order to account for this loss.

4.3 TWO LEVEL ACQUISITION

In those applications where integration over many hops is required for satisfactory detection performance, the implementation of matched filters can be formidable since the number of correlators is M, while serial search results in excessively long acquisition times. A possible compromise is to incorporate matched filtering as an

acquisition aid for starting the receiver's code generator at a pre-arranged code phase and then performing active correlation over a longer code segment to confirm coarse alignment. However, a false alarm from the matched filter will engage the active correlator and can prevent recognition of the true code epoch. This leads to the two level scheme of Fig. 4.4.

In this scheme a matched filter with a first threshold is used to detect a relatively short M hop sequence, and will generate code start signals for those hop intervals in which its detection threshold is exceeded. Each code start signal will engage any one of c active correlators that is idle, and cause it to cycle through a sequence of K hops. At the end of the K hops the output of the active correlator is compared with a second threshold and if the threshold is exceeded a synch indication is given, otherwise the correlator is again made available to the common bank.

Now a false synch indication will be given only when all the following occur:

(a) The matched filter generates a false code start signal.

(b) The false code start signal finds at least one active correlator idle.

(c) The active correlator engaged falsely detects the in-synch condition.

We denote the false hit error probability for the matched filter and active correlators as P_{FHM} and P_{FHK} respectively. The matched filter makes a threshold comparison every hop

interval and therefore generates false code start signals at an average rate of

$$R = P_{FHM}/T_H. \tag{4.4}$$

Each code start signal engages an active correlator for KT_H seconds, if at least one is idle. The activity of the bank of c active correlators can be modelled as a queuing system with Poisson arrival, arrival rate R, a finite number of servers, c, and fixed holding time KT_H with no room for waiting. The probability that a code start signal finds all c correlators engaged is then just the blocking probability for this queue. This is given by the Erlang B loss formula, B(c,a), where

$$a = RKT_H = KP_{FHM}, \tag{4.5}$$

and can be conveniently computed using the recursion formula,

$$B(c,a) = aB(c-1,a)/[c+B(c-1,a)] \tag{4.6}$$

beginning with B(0,a)=1. When the false code start signals arrive according to a Poisson process the events (a), (b) and (c) above are statistically independent. Thus the probability of a false synch indication is the product of the probabilities for each event,

$$P_{FA} = P_{FHM}(1-B(c,a))P_{FHK} \quad . \tag{4.7}$$

A message preamble can be missed in any of the following ways:

(a) The matched filter falsely dismisses the M hop synch prefix when it occurs.

(b) The matched filter correctly detects the prefix but finds all active correlators engaged.

(c) The matched filter correctly detects the prefix and finds an idle active correlator, but the active correlator falsely dismisses the correct in-synch condition.

We denote the no-hit error probability for the matched filter and active correlators as P_{NHM} and P_{NHK} respectively. The events (a), (b) and (c) above are mutually exclusive so that the probability of missing the message preamble is the sum of the probabilities for each event,

$$P_M = P_{NHM} + (1-P_{NHK})[B(c,a)+(1-B(c,a))]P_{NHK} \quad . \tag{4.8}$$

Since the two level scheme searches the uncertainty region in real time,

$$N_s = N_u + M + K \quad . \tag{4.9}$$

4.4 EARLY-LATE GATE TRACKING

The early-late gate tracking loop as used for range tracking in radar systems [15] lends itself well to the FH signal application. The diagram of Fig. 4.5a shows the system required to track FH signals, while Fig. 4.5b shows the waveforms associated with the early-late gate control loop. The gating waveform g(t) derived from the VCO is alternately positive and negative with plus and minus transitions coinciding with the edge and centre of the frequency hopping intervals in the locally generated FH waveform $S_L(t)$. The detected correlator output v(t) is essentially multiplied by this gating waveform and the result u(t) integrated to form the error signal e(t). This error signal will then be proportional to the delay τ between the local and received FH waveform according to the discriminator characteristic in Fig. 4.5b, and is used to advance or retard the local waveform into alignment.

Inherent in the loop operation will be some phase jitter which will increase with decreasing signal-to-noise ratio. The variance of this phase error is given in [15] for a single received pulse as,

$$\sigma_\phi^2 = T_g T_p / (8E_p/N_o) \quad , \qquad (4.10)$$

where T_g is the gating interval, T_p is the pulse width, and E_p is the pulse energy. For the FH system early-late gate,

T_g equals the hop interval T_H, while T_p equals T_H+T_M. Hence

$$\sigma_\phi^2 = T_H(T_H+T_M)/(8\gamma E_H/N_o) \ , \qquad (4.11)$$

where γ is the number of hops in the loop integration time. This result agrees with that in [16] with $T_M=0$ and the loop bandwidth written as $B_L=1/\gamma T_H$.

In addition to providing a fine control for accurate synchronization of receiver and transmitter, it is also necessary, once the system enters the lock state, to monitor whether or not tracking of the correct received code phase is taking place. This is the purpose of the in-lock detector included in Fig. 4.5a. Depending on the lock mode control strategy, one or more failures of the lock detector integrator output to exceed the threshold will indicate loss of lock and return control to the search mode.

Tracking loop phase error will reduce signal correlation thereby degrading in-lock detector performance, and this must be accounted for as follows. Since the phase error is approximately Gaussian [16], it will be less than $3\sigma_\phi$, 90 percent of the time. It can then be seen from the diagram of Fig. 4.5d that correlation is reduced by a factor less than $3\sigma_\phi/T_H$ so that signal energy must be scaled by a factor greater than,

$$d_t = (1-3\sigma_\phi/T_H)^2 \ . \qquad (4.12)$$

5. RESULTS FOR SOME EXAMPLE SYSTEMS

5.1 A FAST ACQUISITION SYSTEM FOR MOBILE USE

As a first example we consider a system for use in a vehicle configuration for medium range mobile tactical communications. Operators are assumed to communicate in a push-to-talk mode, synchronization being initiated with every transmission. A fast and reliable acquisition system is therefore required. Medium range communications networks operate typically in the VHF frequency range, where tropospheric scattering is not of concern. The most serious threat to mobile units is enemy jamming, against which FH is used as a counter measure. Our design philosphy is therefore dictated by the need for reliable acquisition in the face of such a threat.

Since for vehicle configurations space and power limitations do not cause too much of a problem, we consider the use of a matched filter for coarse acquisition, together with an early late gate and in-lock detector for fine acquisition and tracking. The S/L strategy chosen for this example is the simple strategy of Fig. 5.1. For this case,

$$P_L = p_s \ . \tag{5.1}$$

Since acquisition is achieved by the detection of some code prefix, probably buried in an initial header, there is only one opportunity for correct synchronization. False alarms

will cause entry into the tracking mode which incurs a time penalty and may result in the true synch prefix being missed. The probability of false alarm must therefore be kept small, and provided the miss probability is low, radio operators' procedure can accommodate the rare miss. Applying equation (2.25) we find that,

$$T_D = T_H(1+T_{FL}P_{FA}) \tag{5.2}$$

where

$$T_{FL} = \mu/q_1 \ .$$

The first design task is to select the matched filter complexity requirement. Consider the curves of Fig. 5.2 which show miss probability vs energy per hop to noise density ratio for various filter complexities using linear integratiion. It should be noted that each point on the curves is calculated for a fixed false alarm probability. It can be seen that a miss probability of less that 10^{-3} is achieved for M=4 at a 10dB signal to noise ratio, which we shall deem to be adequate.

As discussed in section 2.3, binary integration offers better performance than linear integration in a jamming environment. But what are the tradeoffs? We consider a matched filter with N=4, M=1. In order to establish a setting for the second threshold, we plot miss probability vs the second threshold for various P_{FA} (i.e. first

threshold) as shown in Fig.5.3. Here, and in general it was found that the optimum setting is the nearest integer to

$$L = (N+0.5)/2 \ . \qquad (5.3)$$

The curves of Fig. 5.4 and Fig. 5.5 demonstrate the trade-off in performance in a benign environment for interference immunity. When there is no interference, binary integration is about 1.5dB inferior to linear integration, whereas binary integration is superior when the interference to signal ratio exceeds about -1dB with 1% of the band jammed.

Finally, we wish to determine the effect of the jamming environment on tracking performance. The curves of Fig.5.6 compare the predicted mean time to loss of lock vs energy per hop to noise density ratio for the benign environment, and when 10% of the hopping band is jammed. It should be noted that each point on the curves is calculated for a given mean time to reject a false lock. Hence the effect of a jamming environment is to force an increased threshold level in order to maintain a fixed T_{FL}, reflected in the results by a reduction in T_{LL}. As can be seen from the curves, the effect of jamming when binary integration is used is minimal, whereas when linear integratiion is used the effect is quite severe. An actual time scale is provided for the example of a hop rate equal to 100 hops per second and adequate performance is obtained.

5.2 A COMPACT SYSTEM FOR HAND-HELD USE

We next consider the application of a hand-held radio for use in an urban environment, operating typically in the UHF range. In this context FH modulation is utilized mainly for its multiple access capability and its inherent ability to counter the multipath problems associated with this environment.

Due to size and power limitations the introduction of the more complex acquisition schemes is precluded, and we are led to a choice of the serial search scheme for coarse acquisition. Combining this with the early-late gate tracking scheme results in the relatively compact system of Fig.5.7. A possible synch procedure here is to gain acquisition over a subset of the frequency hop set in order to produce realistic acquisition times. The early-late gate is needed more here for fine acquisition than tracking, since transmissions are generally very short.

One of the advantages of serial search is the versatility of choice in search strategy, while its main disadvantage is longer acquisition times. It is possible however, by the careful choice of search strategy and by maintaining a short uncertainty region, to keep acquisition time to a minimum. We therefore compare several strategies in terms of 90^{th} percentile acquisition time. The

strategies considered are shown in Fig.5.8. The scheme in (d) is the 'double dwell' strategy in which the second detection integration is extended. In order to make comparison feasible, the following criterion is applied:

$$\lim_{p \to 1} T_D = 4+k = \text{const} . \qquad (5.4)$$

Applying equation (2.32) we find that the probability of lock for the various schemes is:

$$\begin{aligned} &(a) \quad P_L = p \\ &(b) \quad P_L = p^4 \\ &(c) \quad P_L = p^4/[1-3pq+p^2q^2] \\ &(d) \quad P_L = p_1 p_2 . \end{aligned} \qquad (5.5)$$

Applying equation (2.34) we find that the mean dwell time for the various schemes is:

$$\begin{aligned} &(a) \quad T_D = 4+pk \\ &(b) \quad T_D = 1+p+p^2+p^3+p^4k \\ &(c) \quad T_D = [1+p+p^2+p^3+p^4k]/[1-3pq+p^2q^2] \end{aligned}$$

(d) $T_D = 1+3p_1+p_1p_2k$

(5.6)

Consider the curves of acquisition time vs probability of false alarm in Fig.5.9 for each of the strategies in Fig.5.8. In each case there is an optimum value for P_{FA} for minimum acquisition time at the chosen signal to noise ratio. A high probability of false alarm results in a long average dwell time, while a low probability of false alarm implies a high threshold and hence a high miss probability. These results are utilized in the comparisons to follow. It should be noted that acquisition time has been normalized to N_u.

Consider next the curves of Fig.5.10 which plot miss probability vs energy per hop to noise density ratio for the chosen strategies. The simple strategy is seen to afford the best detection performance. However, on observing the curves of Fig.5.11 which compare the acquisition time performance of the example strategies, we find that the simple strategy is no longer the best. As expected, strategy (a) yields poor results, but it is interesting to note that while strategies (b) and (c) yield similar performance strategy (d) provides a marked improvement.

While we might have been persuaded to choose strategy (d) for the best performance in a benign environment, the curves of acquisition time vs fraction of hopping band occupied in Fig.5.12 show that in a multiple access environment this strategy is not the best. In this

situation strategy (b) turns out to be relatively interference immune.

Finally, considering the curves of Fig.5.13 which show acquisition time performance of the various strategies for an increasing hop rate, we find that in a multipath environment strategy (d) again out performs the others. As can be seen, hop period should not be smaller than the channel multipath spread, otherwise performance becomes seriously degraded.

5.3 A ROBUST SYSTEM FOR BASE STATION USE

As a final example let us consider a system for use in a long distance base station communication link. Such systems operate generally in the HF frequency band, relying on troposcattr reflections for beyong the horizon ranging. The effect of fading is thus of prime importance in the design of a synchronization system.

The role of the base station communication link demands high security in order to combat interception by frequency hopping pattern decoding. A time of day reference is possibly established by an initial synchronization procedure, with subsequent coarse acquisition at the start of each transmission compromising a search through a code uncertainty region caused by clock instability. Late entry (newcomers to the network) is achieved by searching an

uncertainty region relative to the time of day reference. The coarse acquisition system is therefore required to rapidly and reliably search through a given code uncertainty region in a signal subject to fading. Since space and power limitations are of secondary importance we consider the use of the two-level scheme for this application.

Tracking is once again performed by the early late gate and monitored by the in-lock detector. However, due to the possible occurrence of deep fades we shall investigate the use of the consecutive count lock strategies shown in Fig.5.14. This comparison is done according to the following criterion:

$$\lim_{q \to 1} T_{LL} = m(n+1) = \text{const.} \tag{5.7}$$

The generalized graph transfer function for Fig.5.14 is obtained by inspection using Mason's formula [12] as

$$P(z) = q^{n+1} z^{n+1} / (1 - pz \sum_{i=0}^{n} q^i z^i) \ . \tag{5.8}$$

Applying equation (2.40) and using p=1-q it is found that

$$T_L = MT_H (1-q^{n+1}) / [(1-q) q^{n+1}] \ . \tag{5.9}$$

Two-level acquisition performance is demonstrated by the curves of Fig.5.15, which show miss probability vs energy per hop to noise density ratio for a varying number of active correlators. The advantage to be gained in going

from one to two active correlators is evident. However, it is likely that the extra complexity for four correlators would not be warranted in the benign environment.

Turning now to the curves of Fig.5.16 which show miss probability vs relative strength of scatter component, again for a varying number of active correlators, we find that the fading channel severely affects performance, and for the chosen integration parameters M and k, the extra active correlators are warranted.

The fading environment is also likely to have a serious effect on tracking performance. But first let us consider the difference in performance for the chosen strategies, as depicted in the curves of Fig.5.17. It is comforting to find that there is little loss in performance incurred for trading detector integration time against the number of in-lock states. Sample times given are for a hop rate of 10 hops per second, considered as reasonable for the HF band. The curves predicting performance in a fading channel indicate the severe effect of such an environment. In order to improve on this situation it is necessary to increase the in-lock detector integration time. However this must be done subject to the constraint

$$M(n+1) < \lim_{q \to 1} T_L \ . \qquad (5.10)$$

6. CONCLUSIONS

6.1 COMPARISON OF COARSE ACQUISITION SCHEMES

In the course of selecting an acquisition scheme for application in each of the example scenarios in section 5, an attempt has been made to choose common parameter values, in particular the false alarm probability. This enables us to compare the performance of each of the schemes outlined in section 4.

Let us compare the curves of Fig.5.2, 5.10 and 5.15. Clearly the matched filter offers better detection performance than the serial search scheme. This is due to the ability of the matched filter to find the peak correlation with the correct code phase in the received waveform. In addition, the way in which the matched filter searches the received code in real time provides a speed advantage over stepped serial search at the cost of extra complexity. Techniques such as fast hop search and the double dwell strategy can yield a considerable increase in search rate for serial search, at the cost of detection performance. If the search process can accommodate one or more code epoch detection misses, the serial search scheme utilizing these techniques can provide adequate performance for low complexity.

For the same matched filter complexity the two level scheme yields extremely reliable detection performance, provided that a bank of three or more active correlators is

used for code start signal verification. This, of course, is at the cost of considerable complexity.

6.2 TRACKING IN ADVERSE ENVIRONMENTS

Consider the curves of Figs.5.6 and 5.16. Once again common parameters, in particular the mean time to reject a false lock, have been chosen in order to make comparisons of performance in different environments possible.

The best performance in terms of mean time to loss of lock is obtained by linear integration with a simple strategy. However, the jamming environment was found to seriously degrade performance when this strategy is used. The use of binary integration with the simple strategy was then shown to sufficiently overcome the jamming problem.

The fading channel on the other hand was found to cause a severe reduction in mean time to loss of lock for which the only solution is to increase in-lock detector integration time. However this must be done within the constraint of mean time to reject a false lock and may necessitate a lower detector threshold, which implies a longer mean time to determine an out of lock condition. This affects acquisition time and end of message detection. It is felt that the loss of approximately 1dB in performance for going to a more complex in-lock control strategy is warranted for the case of the selective fading channel.

Although not presented in the results for reasons of clarity, there was found to be little difference between 'up down' and 'consecutive count' strategies for in-lock control.

6.3 PRACTICAL CONSIDERATIONS

In the results of section 5, the parameter used as a measure of signal to noise ratio is the energy per hop to noise density ratio. This ratio assumes (section 2) that the IF filter bandwidth is the reciprocal of the hop interval. However, in practical configurations this is generally not the case, unless the data modulation bit rate equals the hop rate, since we cannot specify that the signal be without information modulation during acquisition. It is the task of the post detection integrator to restrict the noise bandwidth. The energy per hop to noise density ratio is then indicative of the post detection signal to noise ratio.

It will also have been noted that the results predict performance for what is known as a constant false alarm rate receiver. In practice this implies an adaptive threshold, which can generally be achieved by measuring the noise just outside the information bandwidth. However, this measurement will not be indicative of the amount of interference present. A possible solution in the case of the matched filter using binary integration is shown in

Fig.6.1. The threshold input to the digital comparator is derived from the number of frequencies in the prefix simultaneously received, which is an indication of the amount of interference. In this way false alarms are minimized.

APPENDIX A

The ratio of the density function for signal-plus-noise to that for noise alone is the liklihood ratio. This ratio is required to exceed a predetermined threshold value in order to declare that the signal is present. The liklihood ratio is given by (2.6) divided by (2.5),

$$L(v) = e^{-M\varepsilon_i^2/2} \prod_{i=1}^{M} I_o(v\varepsilon_i), \qquad (A.1)$$

where ε_i is the ratio of signal amplitude to rms noise voltage, a_i/σ, and v is the ratio of the IF envelope amplitude to rms noise voltage, r/σ. It is required that

$$L(v) \quad > \lambda \ , \qquad (A.2)$$

where λ is a constant which depends on the probability of a false threshold exceedence. Taking the logarithm gives

$$\sum_{i=0}^{M} \ln I_o(v\varepsilon_i) > \ln \lambda + M\varepsilon_i^2/2 \ . \qquad (A.3)$$

This states that for optimum processing one should take the pulses, each of amplitude r_i, sum them according to the law given by the left-hand side of (A.3), and compare the result with a threshold given by the right-hand side of (A.3). Therefore the detector must have a law given by

$$y = \ln I_0(vs), \tag{A.4}$$

in order to maximize the liklihood ratio L(r) for a fixed probability of false alarm. A suitable approximation for small a_i is the square-law characteristic,

$$y \approx \tfrac{1}{4}(vs)^2, \tag{A.5}$$

and for large a_i a suitable approximation is the linear characteristic

$$y \approx vs. \tag{A.6}$$

APPENDIX B

The mean acquisition time is obtained from Fig. 2.6b as

$$E\{T_{acq}\} = \int_0^\infty tp(t)dt$$

$$= P_D T_S/2 \sum_{n=0}^{\infty} (2n+1)P_M^n$$

$$= T_S[2-P_D]/2P_D \ . \qquad \text{(B1)}$$

Similarly the variance of the acquisition time is obtained as follows,

$$E\{T_{acq}^2\} = \int_0^\infty t^2 p(t)dt$$

$$= P_D T_S^2/3 \ [1 + \sum_{n=0}^{\infty} 3(n+1)nP_M^n]$$

$$= T_S^2[1/3 + 2P_M/P_D + 2P_M^2/P_D^2] \qquad \text{(B2)}$$

and hence

$$var\{T_{acq}\} = T_S^2[1/12 - 1/P_D + 1/P_D^2] \ . \qquad \text{(B3)}$$

APPENDIX C

Consider the correlation diagram of Fig.C1. Let x be the absolute value of the relative delay τ between the transmitter and receiver codes, τ uniform on the time axis. Best correlation occurs for $y=\min(x,2a-x)$. Since x is uniform on $[o,2a)$, y is uniform on $[o,a)$ so that

$$\bar{y} = a/2 \quad \text{and} \quad \overline{y^2} = a^2/3 \ .$$

Considering the stepped search technique, worst case correlation occurs for

$$a = \Delta/2 = T_H(\delta-1)/2 \ ,$$

where Δ and δ are defined by equation (4.2). The correlation output is scaled by $z=1-y/T_H$ so that the signal energy E_H is scaled by

$$d_s = \overline{z^2} = 1 - 2\bar{y}/T_H + \overline{y^2}/T_H^2$$

$$\approx (5-\delta)/4 \ , \quad \delta>1 \ . \qquad \text{(C1)}$$

Considering now the fast hop search technique, we find that there is always some code alignment for which peak correlation in terms of the receiver hop interval occurs. However, the correlator bandwidth has effectively been increased by Δ, so that the ratio E_H/N_o is degraded by

$$d_s = \delta \ , \quad \delta < 1 \ . \tag{C2}$$

Note that this applies to the first signal correlation for each cell only, subsequent correlations being done at the transmitter hop rate. The degradation factors for the examples in Fig. 4.3 are given in Table C1.

REFERENCES

[1] C.R. Cahn, 'Spread Spectrum Applications and State-of-the-Art Equipments',Agard Lecture series No. 58.

[2] R.L. Pickholz, D.L. Schilling and L.B. Milstein, 'Theory of Spread-Spectrum Communications', IEEE Trans. on Comm., Vol. COM-30 No.5, May 1982.

[3] S.S. Rappaport and D.L. Schilling, 'A Two-Level Coarse Code Aquisition scheme for Spread Spectrum Radio,' N.T.C., November, 1979.

[4] C.A. Putman, S.S. Rappaport and D.L. Schilling, 'A Comparison of Schemes for the Coarse Acquisition of Frequency Hopped Spread Spectrum Signals', IEEE Trans. on Comm., Vol. COM-31 No.2, February 1983.

[5] C.A. Putman, S.S. Rappaport and D.L. Schilling, 'Tracking of Frequency Hopped Spread Spectrum Signals in Adverse Environments', MILCOM Conference Record,. October 1982.

[6] A.D. Whalen, 'Detection of Signals in Noise,' New York: Academic Press, 1971.

[7] C.W. Helstrom, 'Statistical Theory of Signal Detection,' London: Pergamon, 1968.

[8] M. Schwartz, 'A Coincidence Procedure for Signal Detection', IRE Transaction On Information Theory, December 1956.

[9] P.M. Hopkins, 'A Unified Analysis of Pseudonoise

Synchronization by Envelope Correlation', IEEE Trans. on Comm. Tech., Vol. COM-25 No. 8, August, 1977.

[10] M. Iosifescu, 'Finite Markov Chains and Their Applications', John Wiley: Romania, 1980.

[11] J.K. Holmes and C.C. Cheng, 'Acquisition Time Performance of PN Spread Spectrum Systems', IEEE Trans. on Comm. Tech. Vol COM-25 No.8, August, 1977.

[12] V.W. Eveleigh, 'Introduction to Control System Design', McGraw-Hill: New York, 1972.

[13] R.S.Kennedy, 'Fading Dispersive Communication Channels', John Wiley: New York, 1969.

[14] S.Stein and J.Jones, 'Modern Communcation Principles', McGraw Hill: New York, 1967.

[15] D.K.Barton, 'Radar System Analysis', Prentice Hall: Englewood Cliffs,N.J., 1964.

[16] M.K. Simon, 'Nonlinear Analysis of an Absolute Value Type of an Early-Late Gate Bit Synchronizer', IEEE Trans. on Comm. Tech., Vol COM-18 No.5, October 1970.

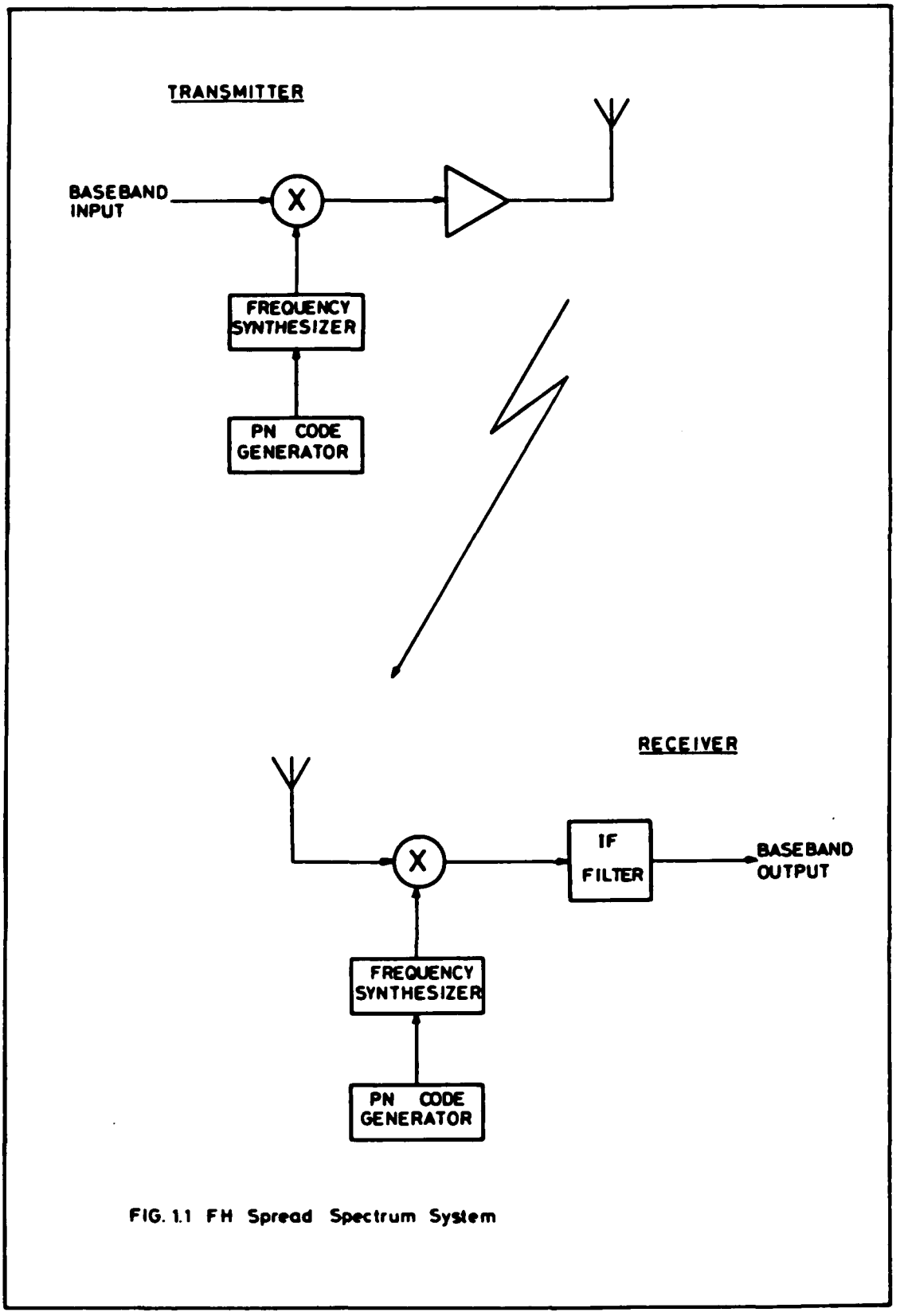

FIG. 1.1 FH Spread Spectrum System

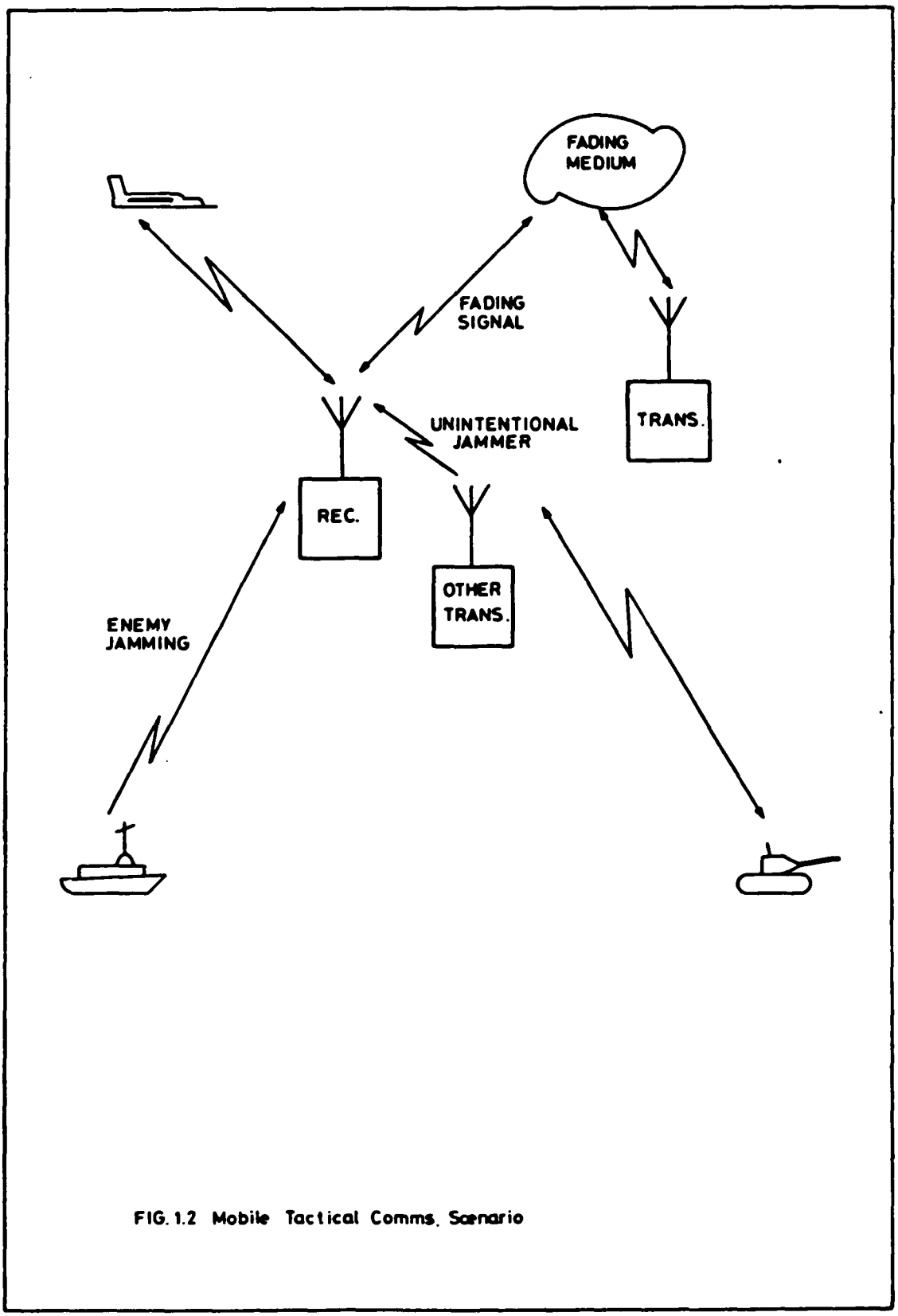

FIG. 1.2 Mobile Tactical Comms. Scenario

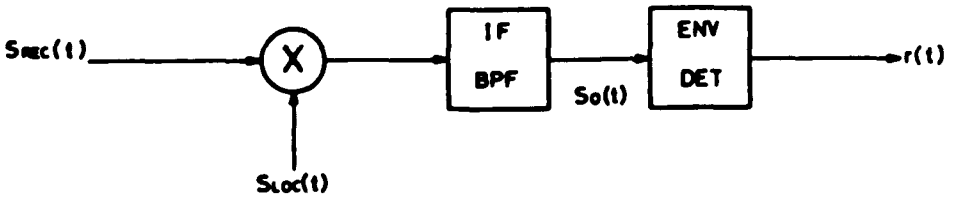

FIG. 2.1a FH Signal Correlation

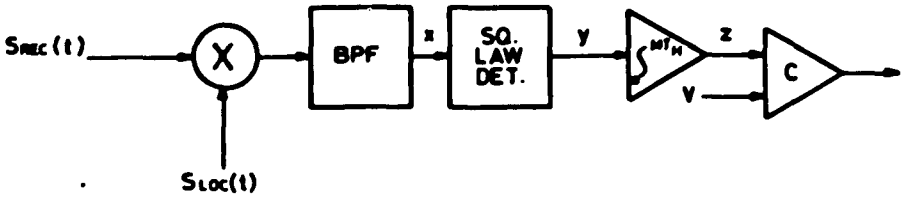

FIG. 2.1b FH Signal Linear Intergration Detection

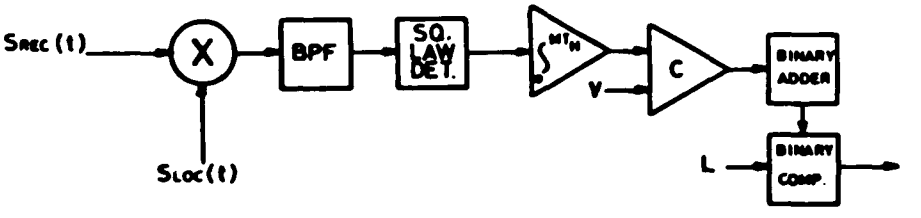

FIG. 2.1c FH Signal Binary Intergration Detection

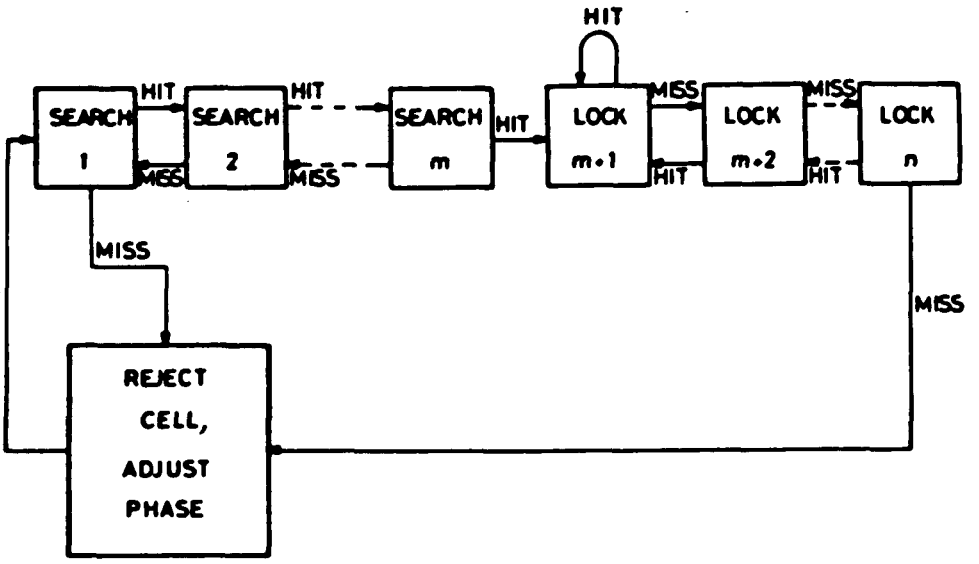

FIG. 2.2a 'Up-Down Counter' S/L Strategy

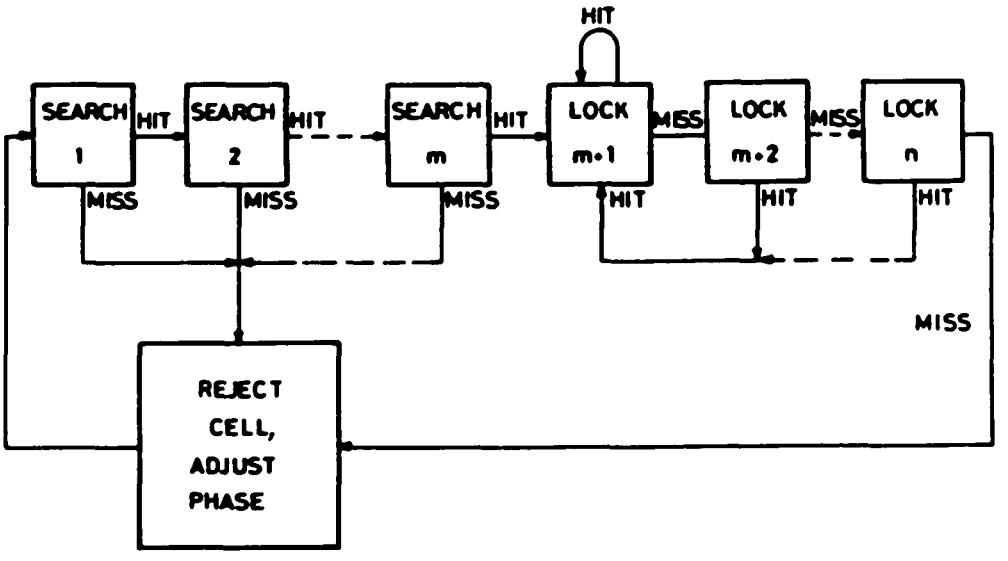

FIG.2.2b 'Consecutive Count' S/L Strategy

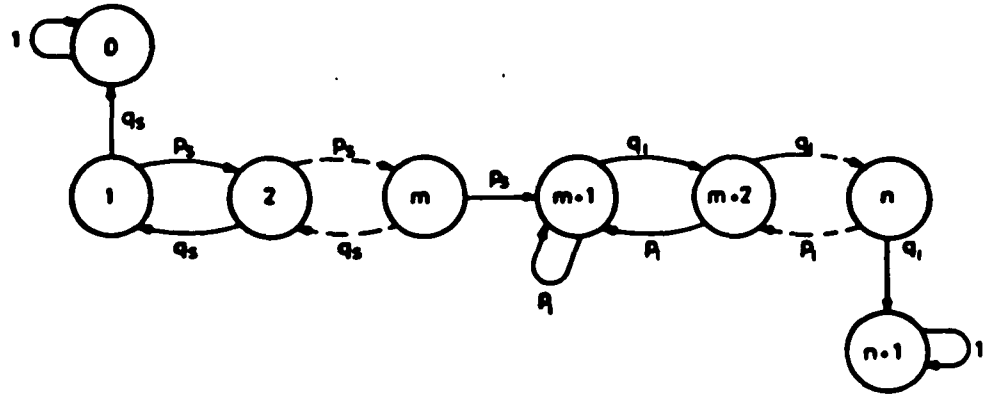

FIG. 2.3a Markov Chain For 'Up-Down' Strategy

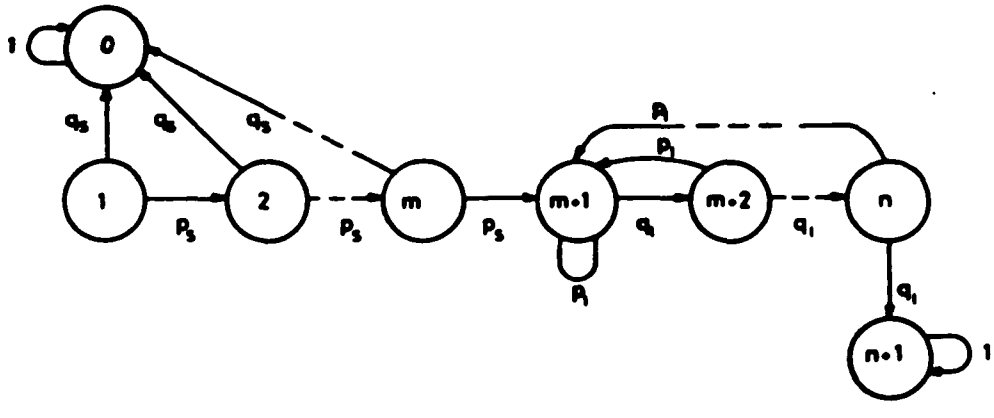

FIG. 2.3b Markov Chain For 'Consecutive Count' Strategy

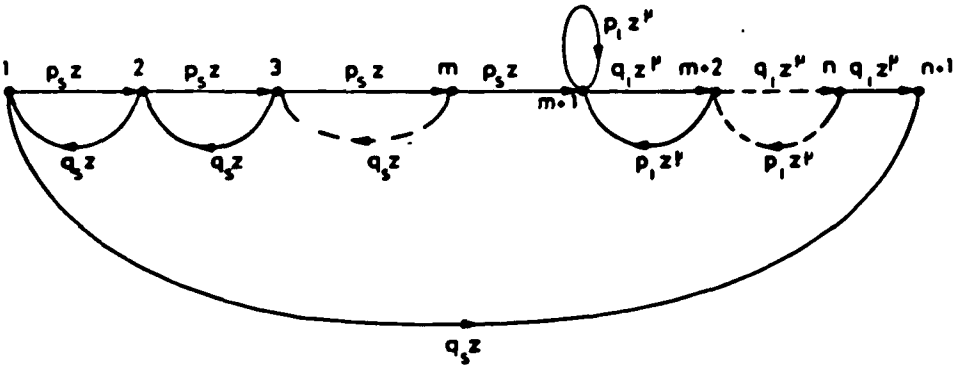

FIG. 2.4 a 'Up-Down Counter' Signal Flow Graph

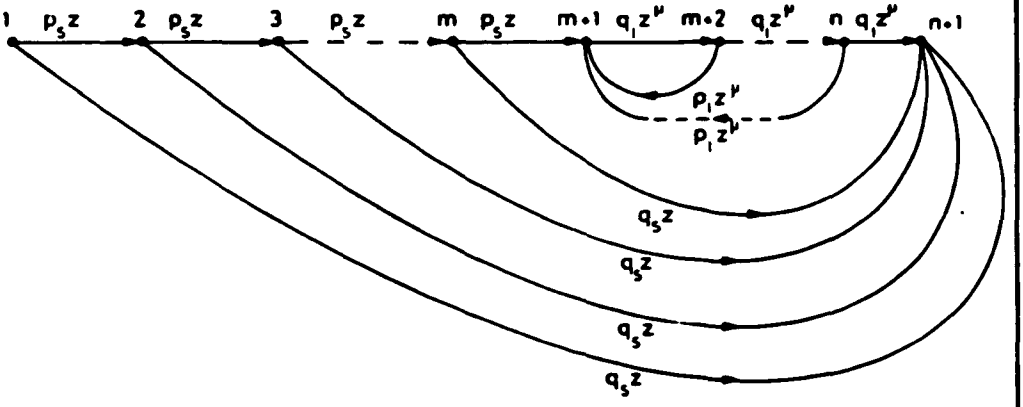

FIG. 2.4 b 'Consecutive Count' Signal Flow Graph

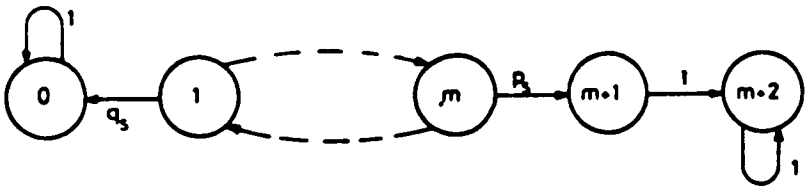

FIG. 2.5a Markov Chain For Search Mode Only

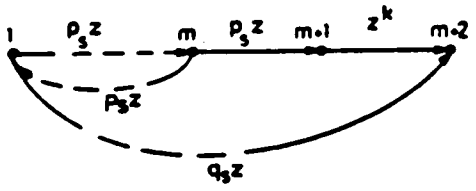

FIG. 2.5 b Signal Flow Graph For Search Mode

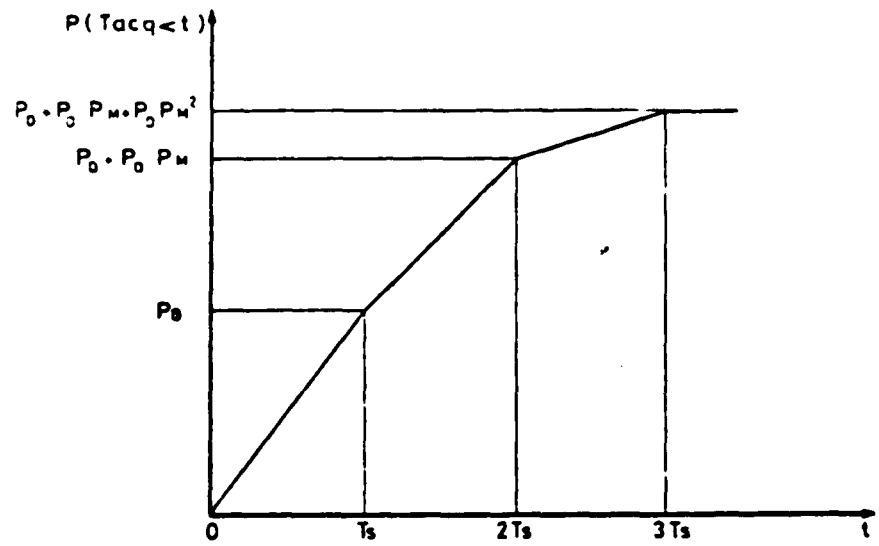

FIG.2.6a Acquisition Time Distribution Function

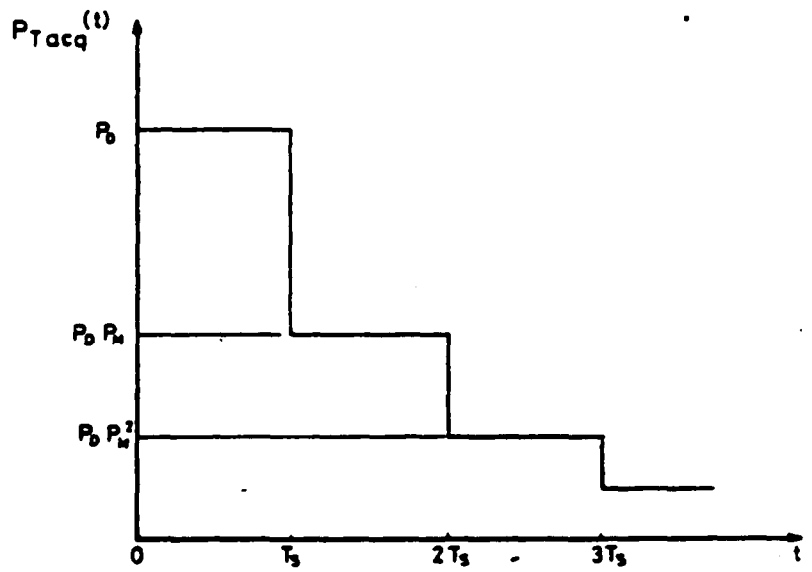

FIG.2.6b Acquisition Time Density Function

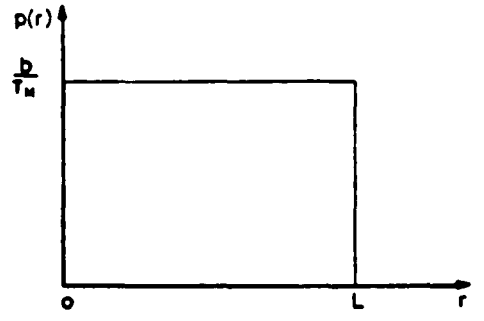

FIG 3.1 a Uniform Scattering Density

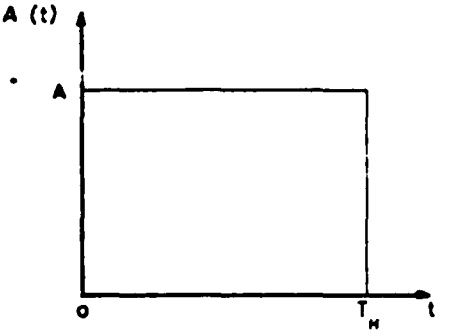

FIG 3.1 b Pulse Amplitude Function

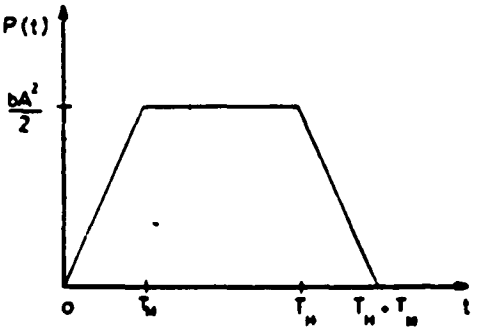

FIG 3.1 c Average Power Function

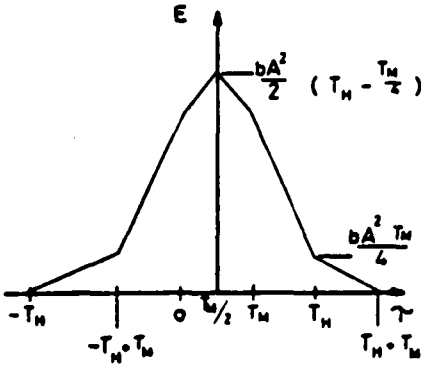

FIG 3.1 d Correlated Energy Diagram

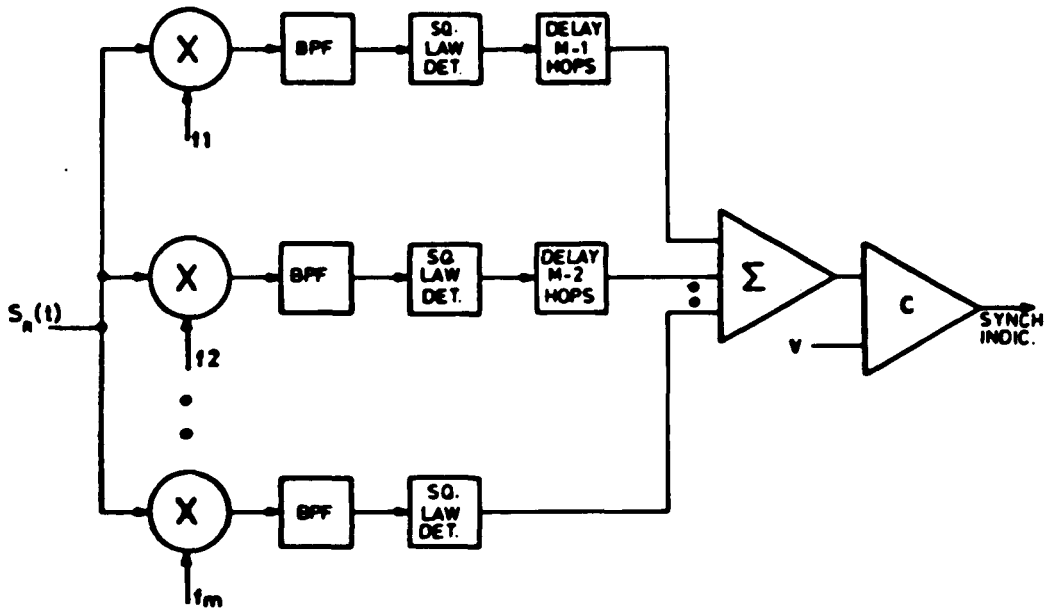

FIG.4.1a Matched Filter Scheme

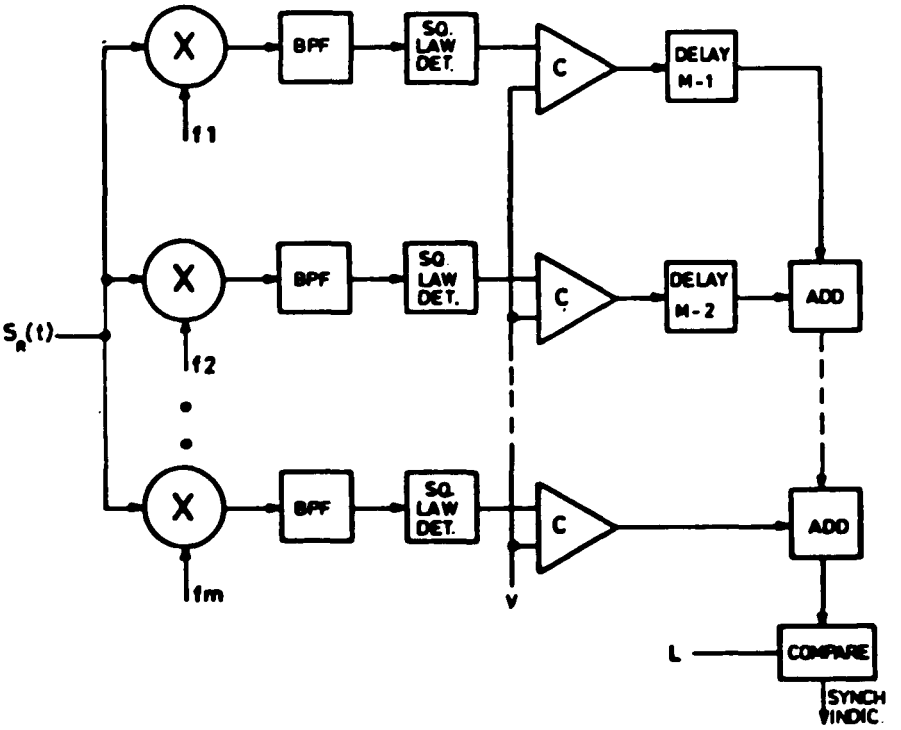

FIG. 4.1 b Quantised Matched Filter

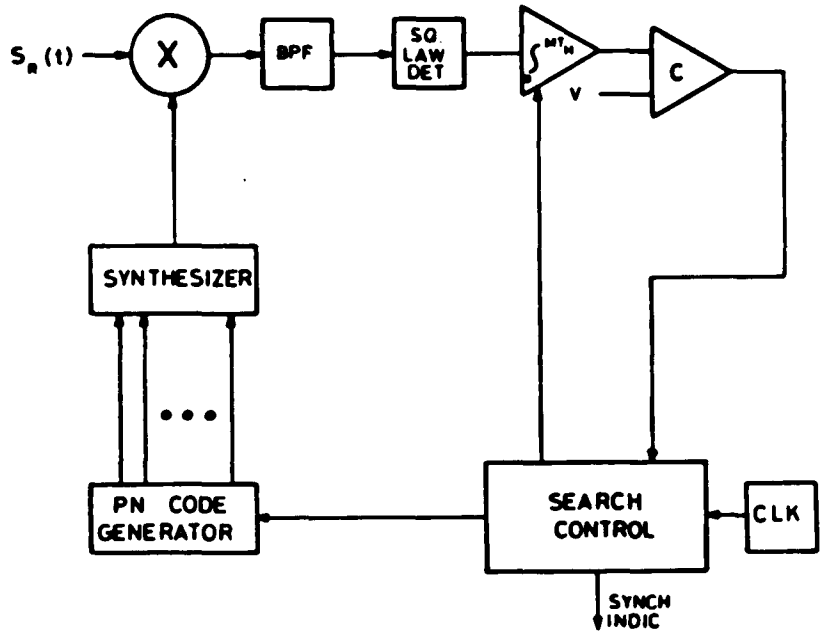

FIG. 4.2a Serial Search Scheme

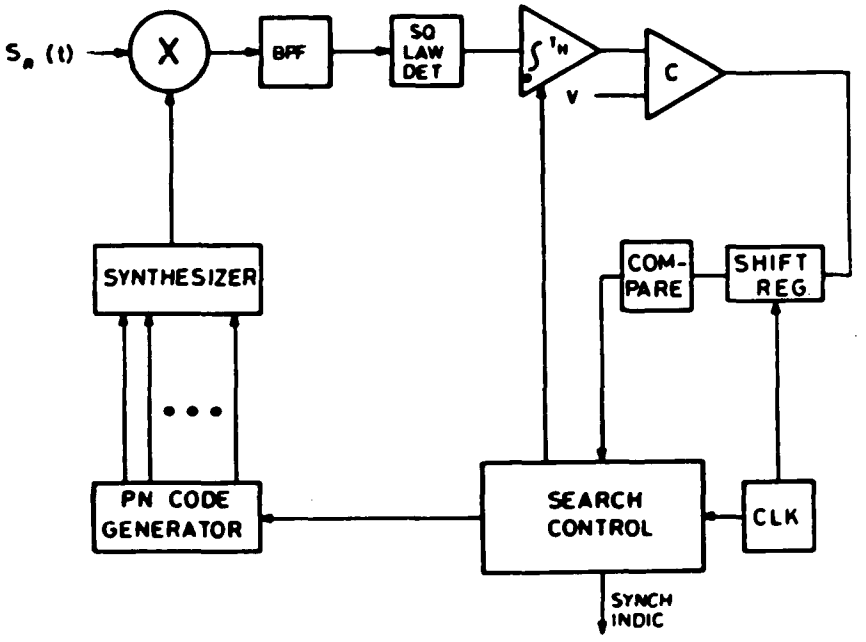

FIG. 4.2b Quantised Serial Search

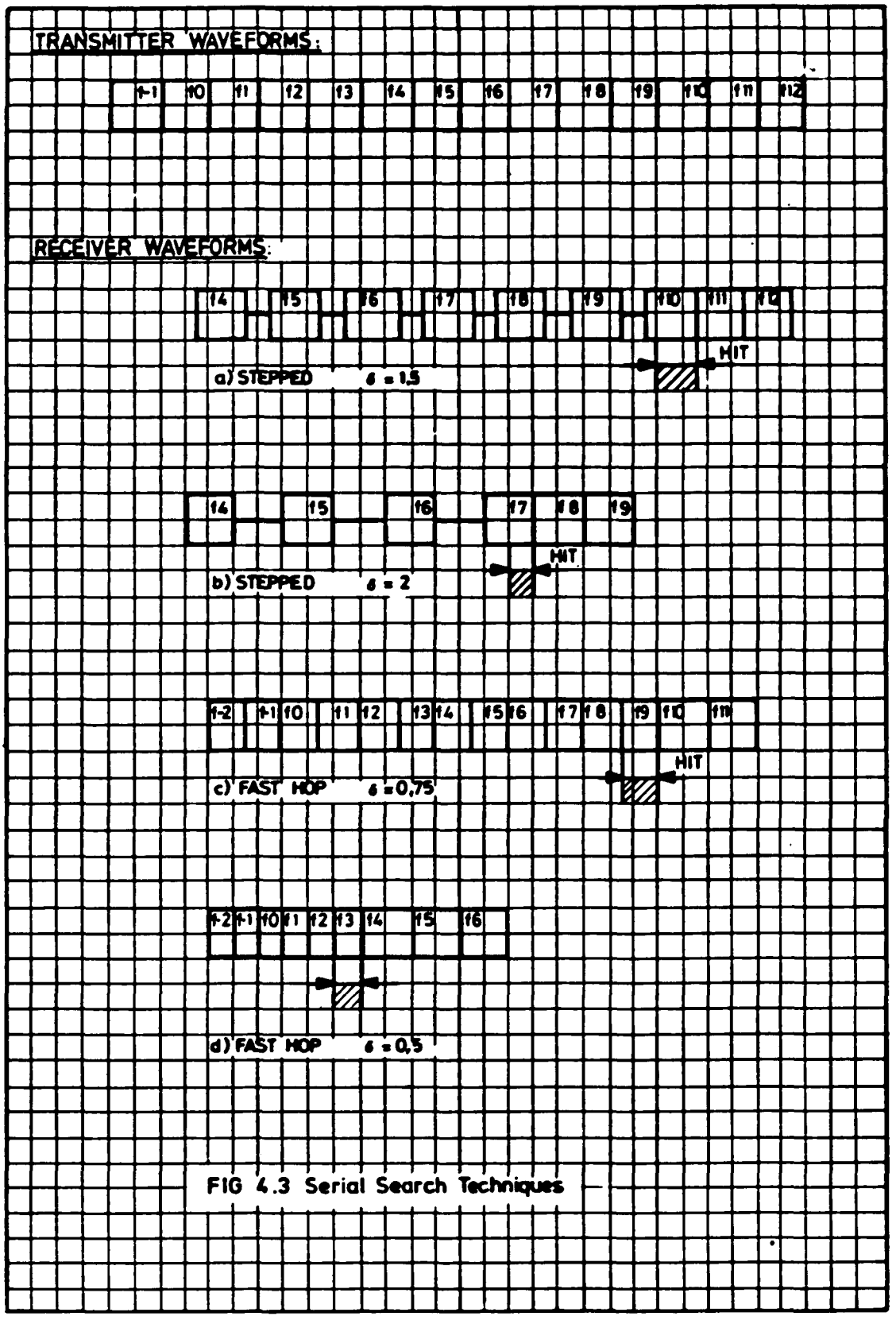

FIG 4.3 Serial Search Techniques

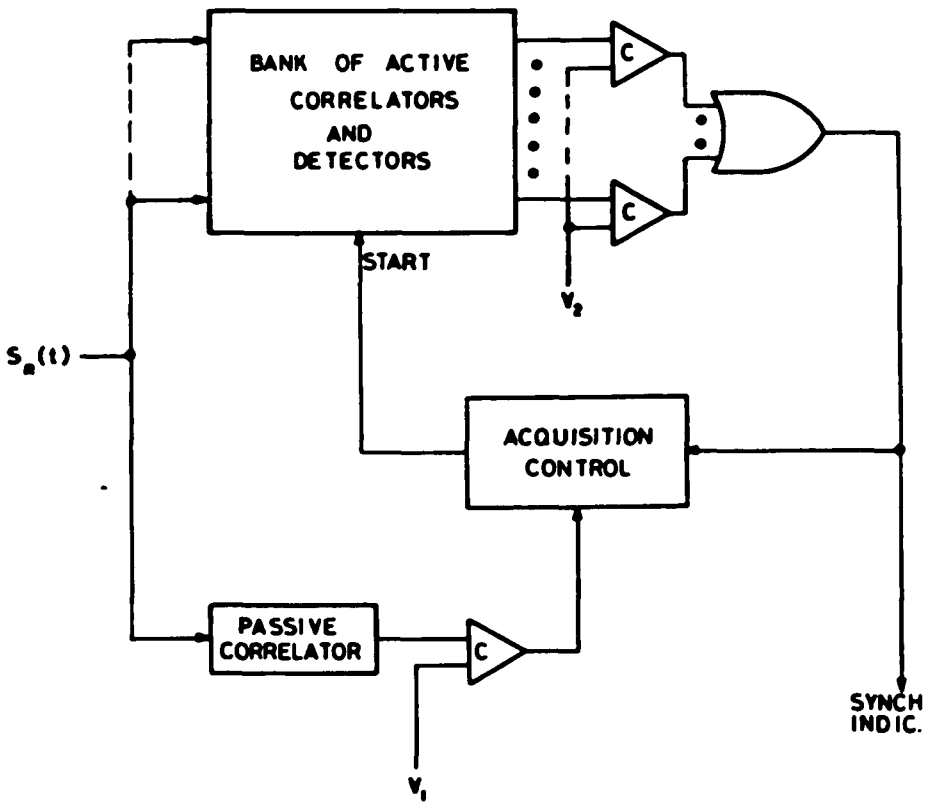

FIG. 4.4. Two-Level Acquisition Scheme

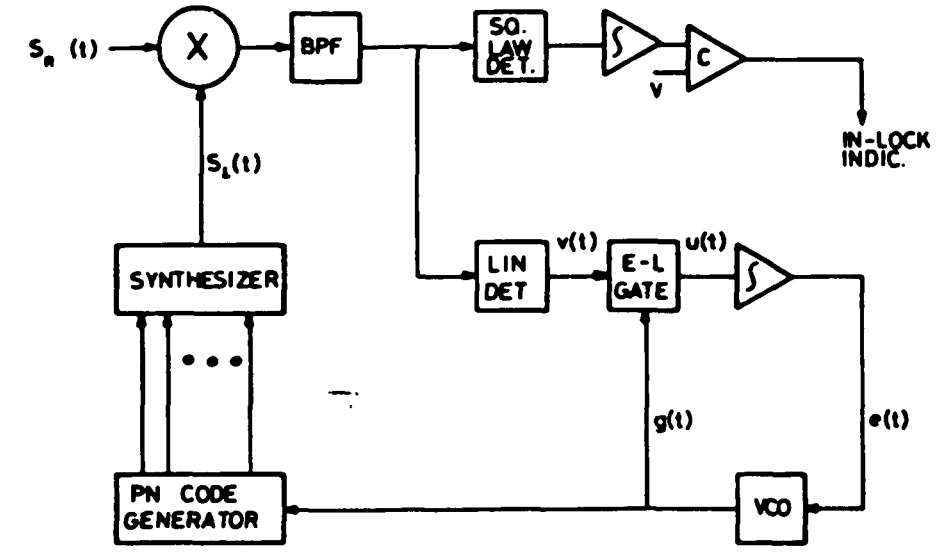

FIG. 4.5a Early-Late Gate Tracking System

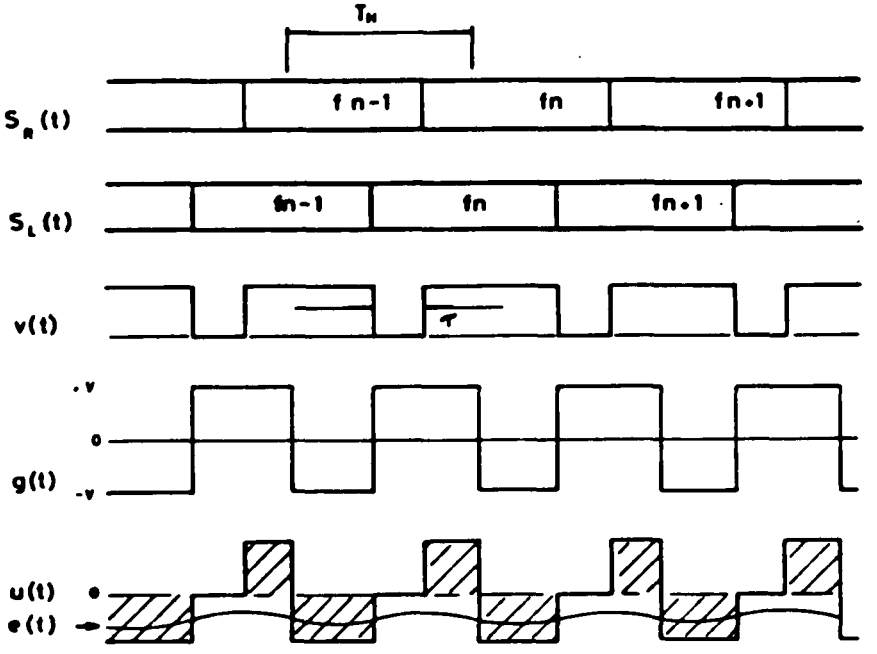

FIG. 4.5 b Tracking Loop Waveforms

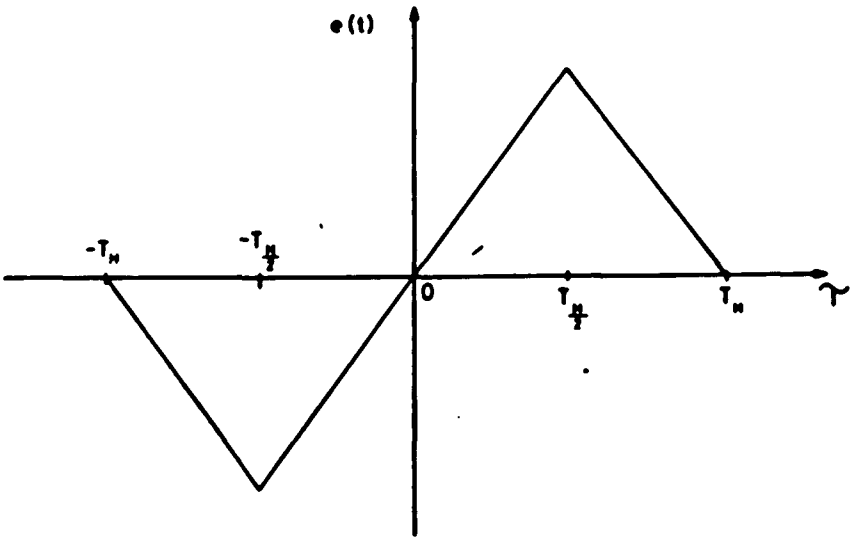

FIG. 4.5c Loop Discriminator Characteristic

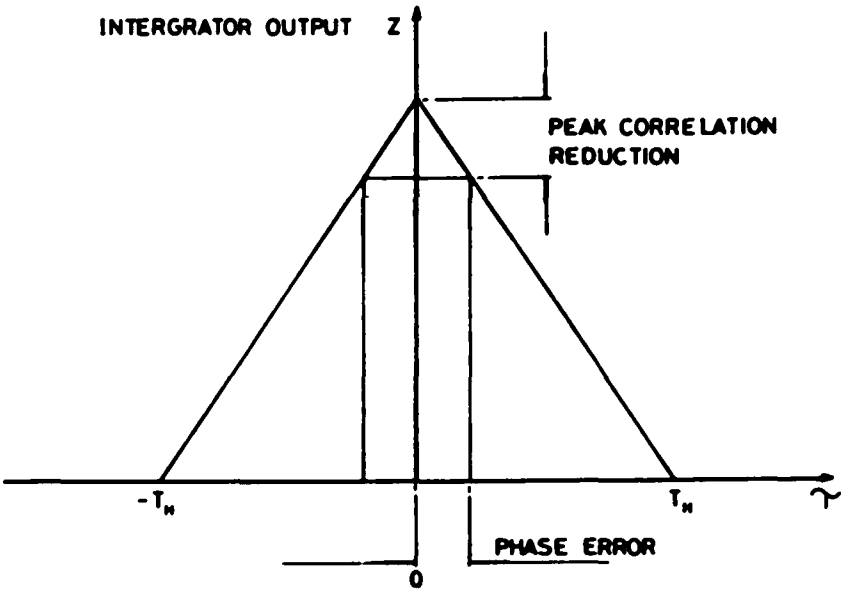

FIG. 4.5d Correlation Diagram

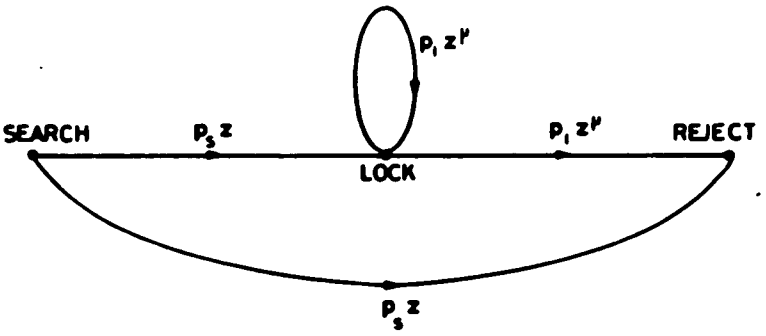

FIG.5.1 Simple S/L Strategy

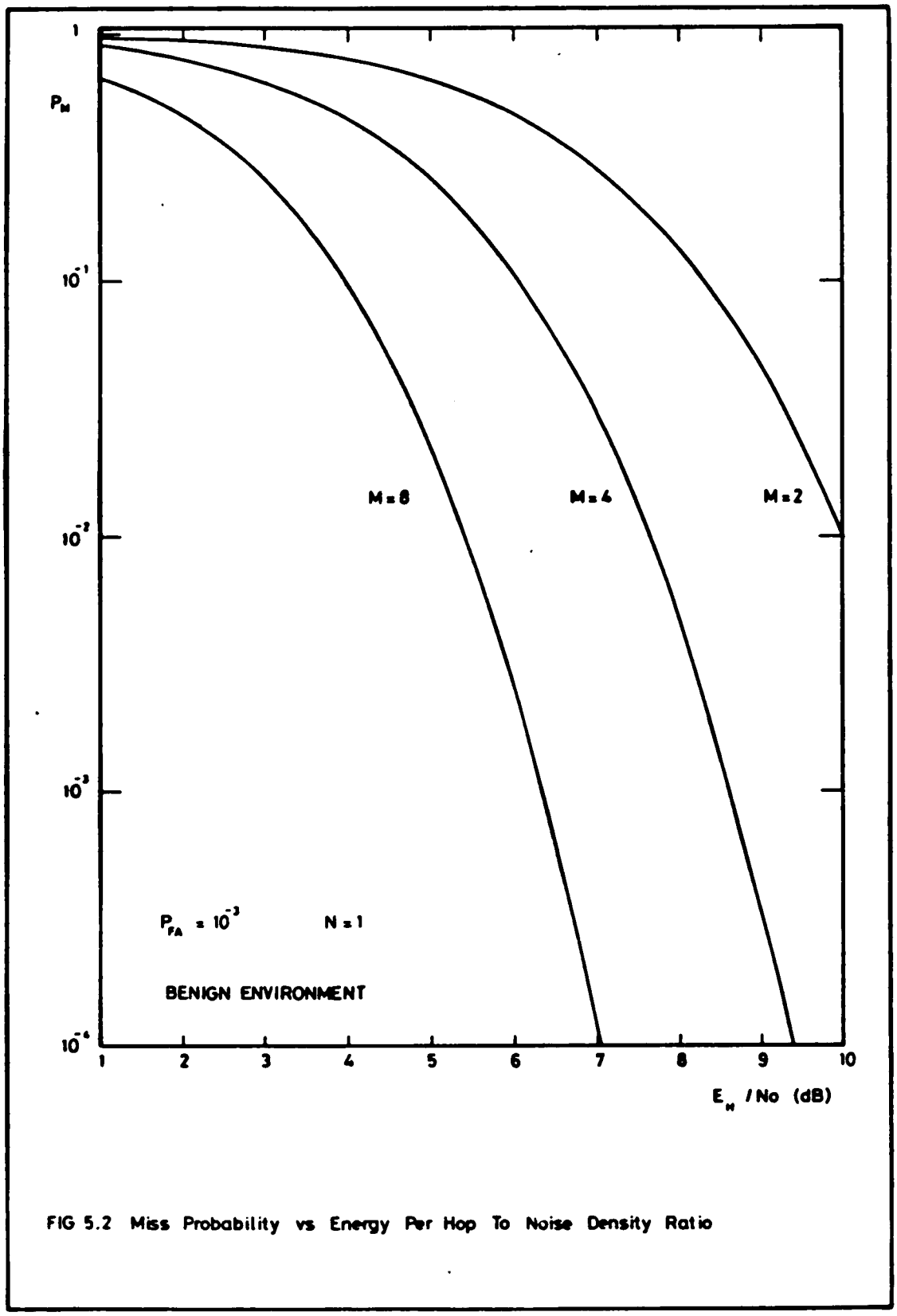

FIG 5.2 Miss Probability vs Energy Per Hop To Noise Density Ratio

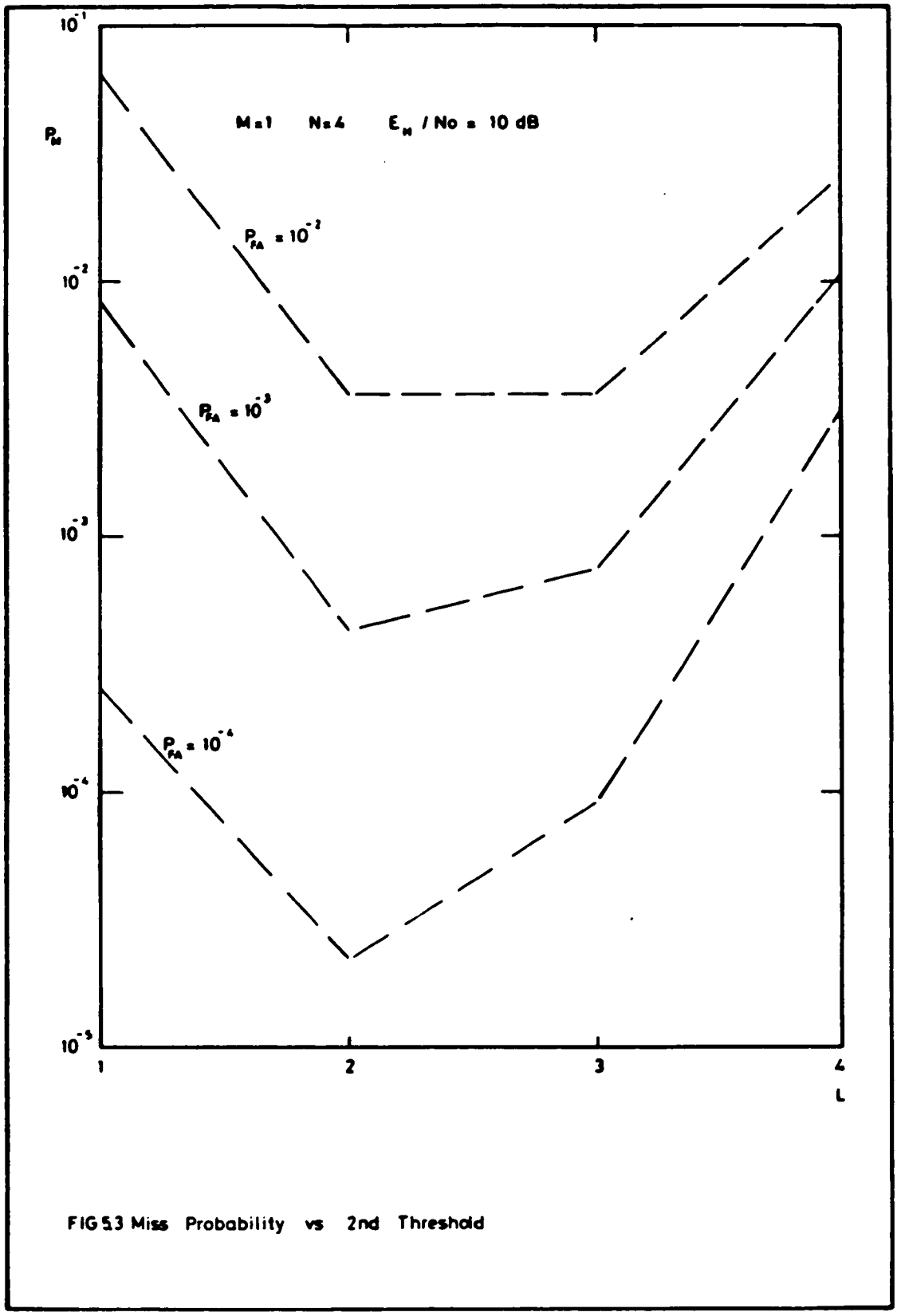

FIG 5.3 Miss Probability vs 2nd Threshold

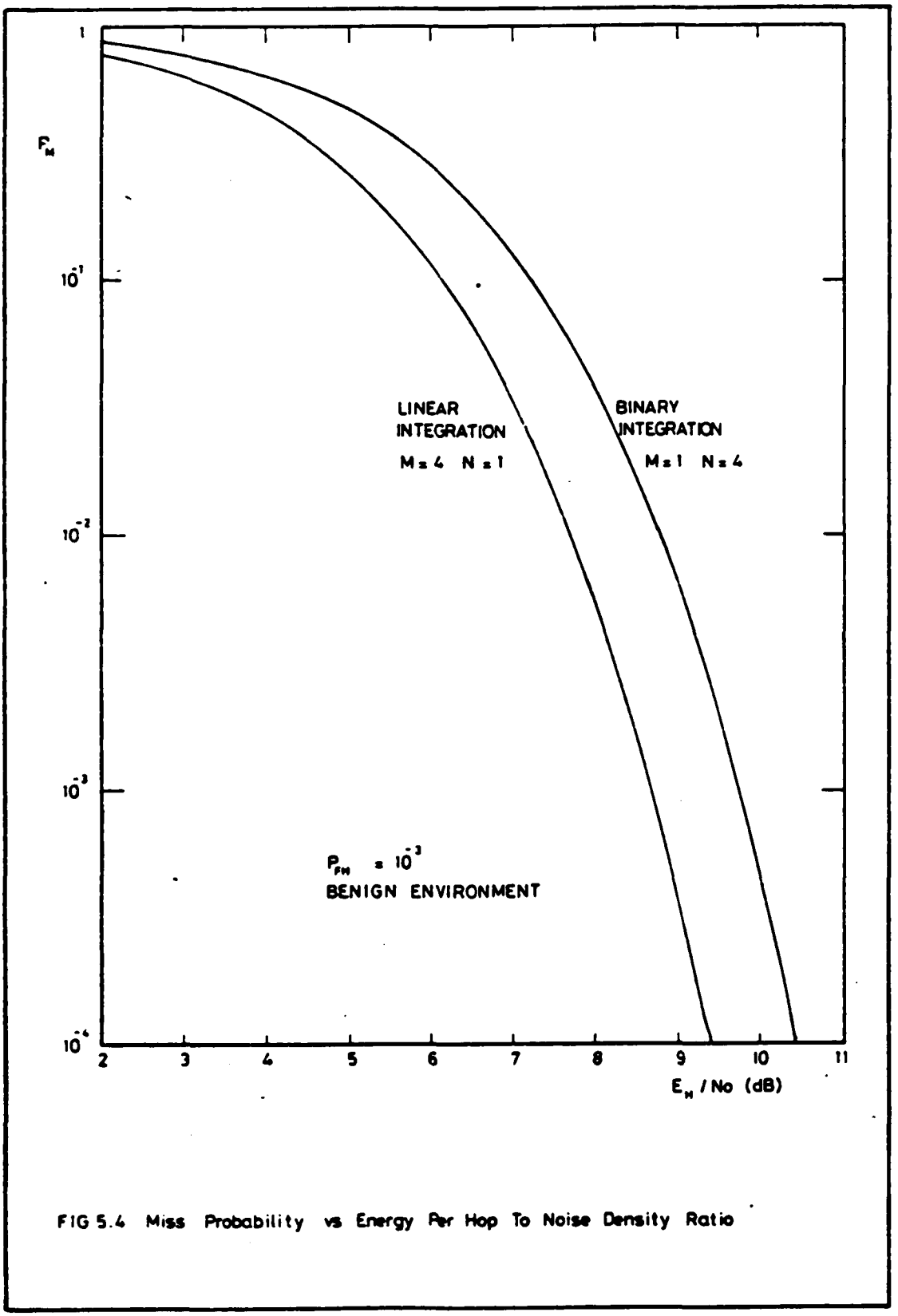

FIG 5.4 Miss Probability vs Energy Per Hop To Noise Density Ratio

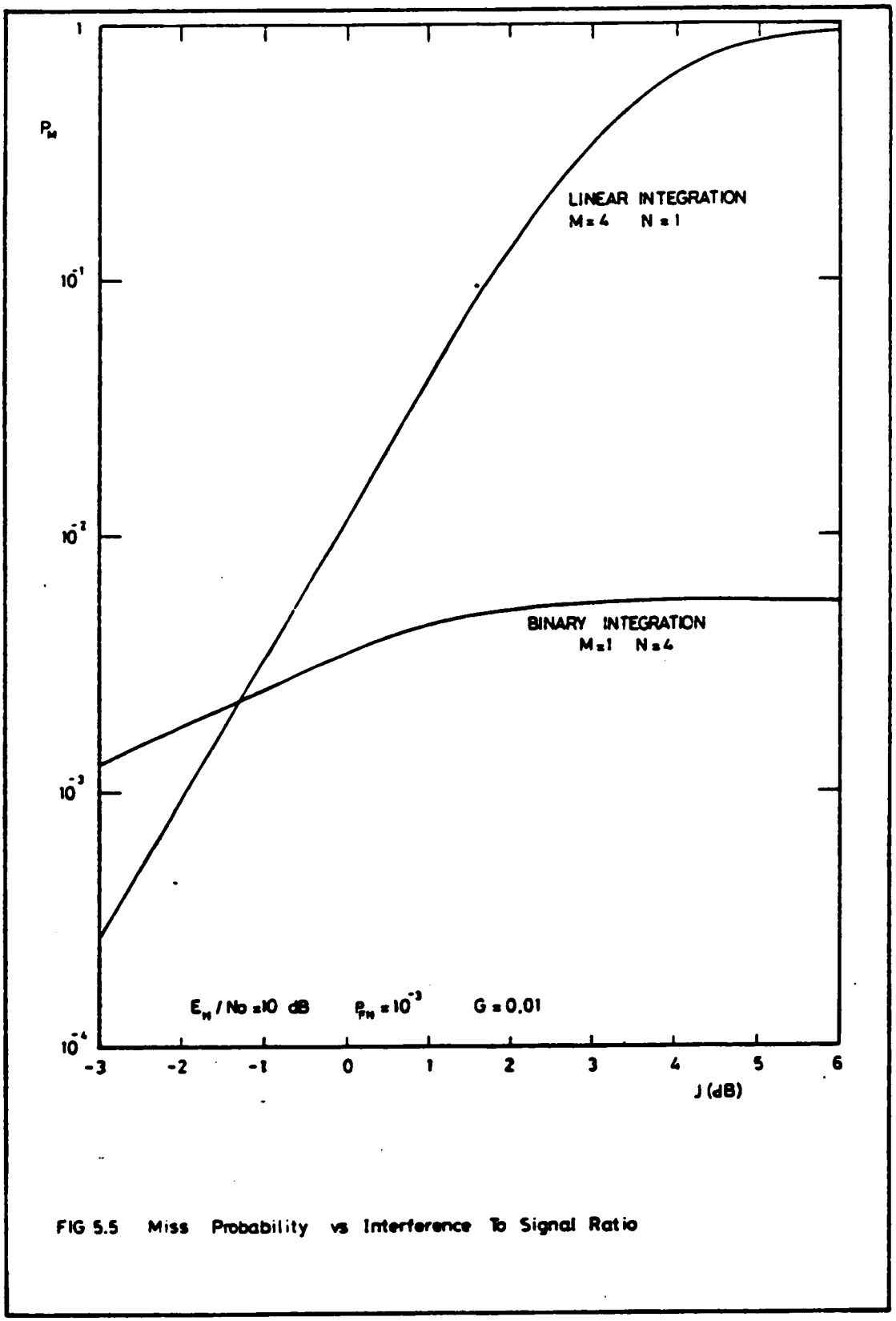

FIG 5.5 Miss Probability vs Interference To Signal Ratio

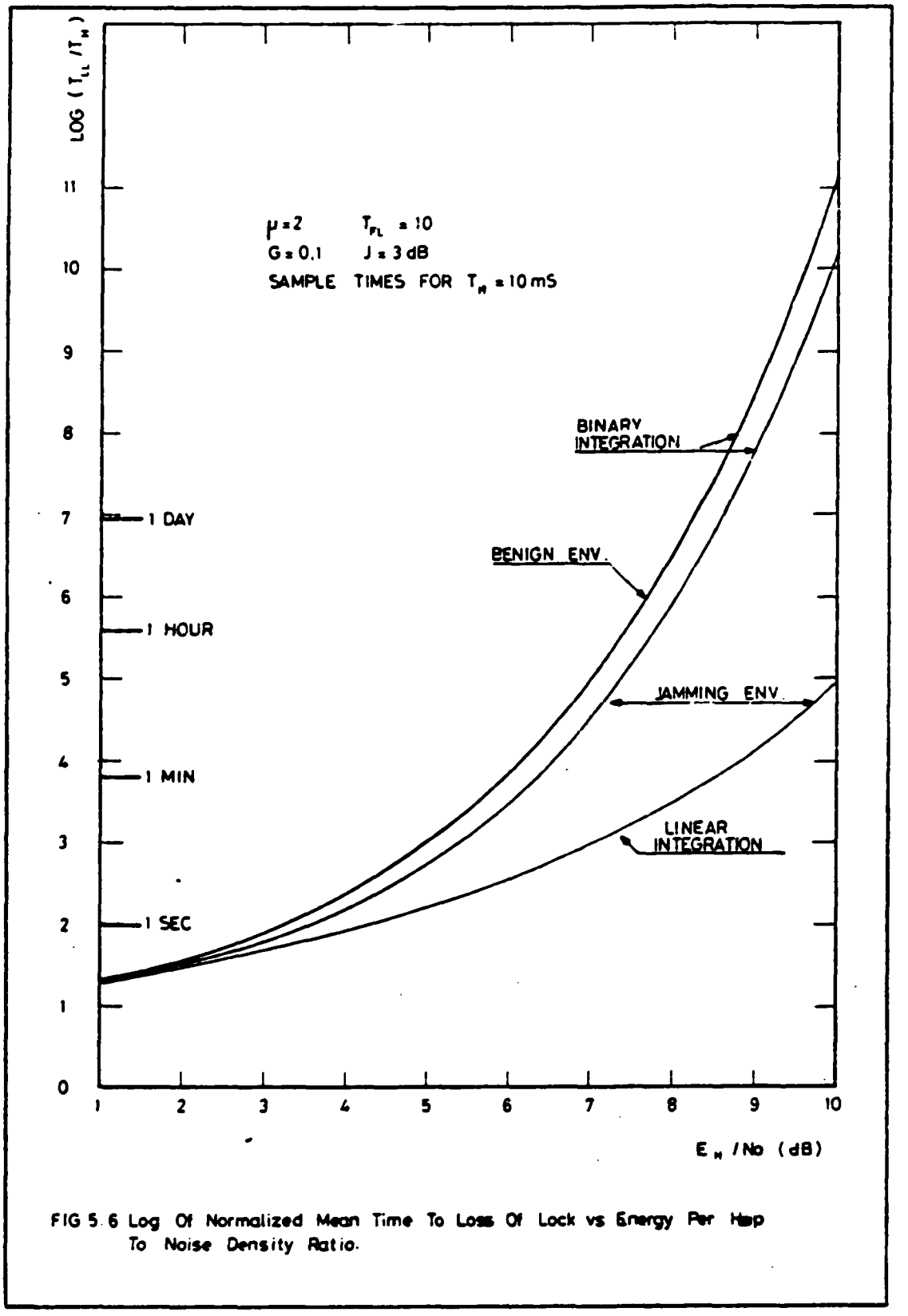

FIG 5.6 Log Of Normalized Mean Time To Loss Of Lock vs Energy Per Hop To Noise Density Ratio.

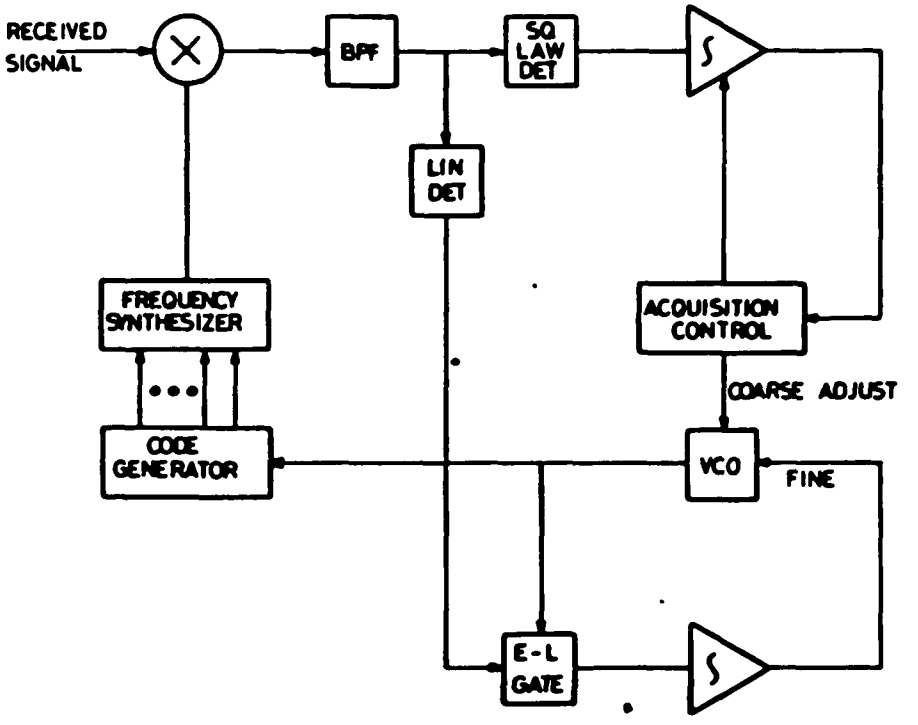

FIG. 5.7 Synchronization System Using Serial Search

a) SIMPLE STRATEGY N = 4 (L = 2)

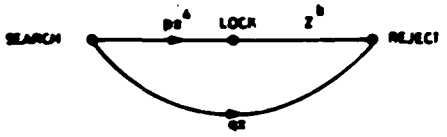

b) CONSECUTIVE COUNT STRATEGY N = 1

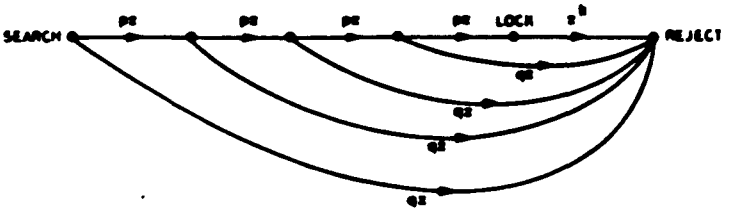

c) UP-DOWN STRATEGY N = 1

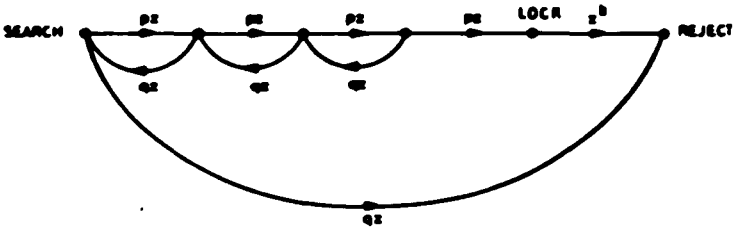

d) DOUBLE DWELL STRATEGY N1 = 1, N2 = 3, (L = 2)

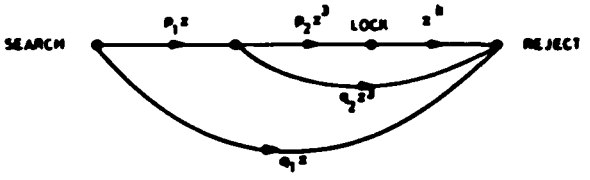

FIG. 5.8. Example Strategies For Serial Search

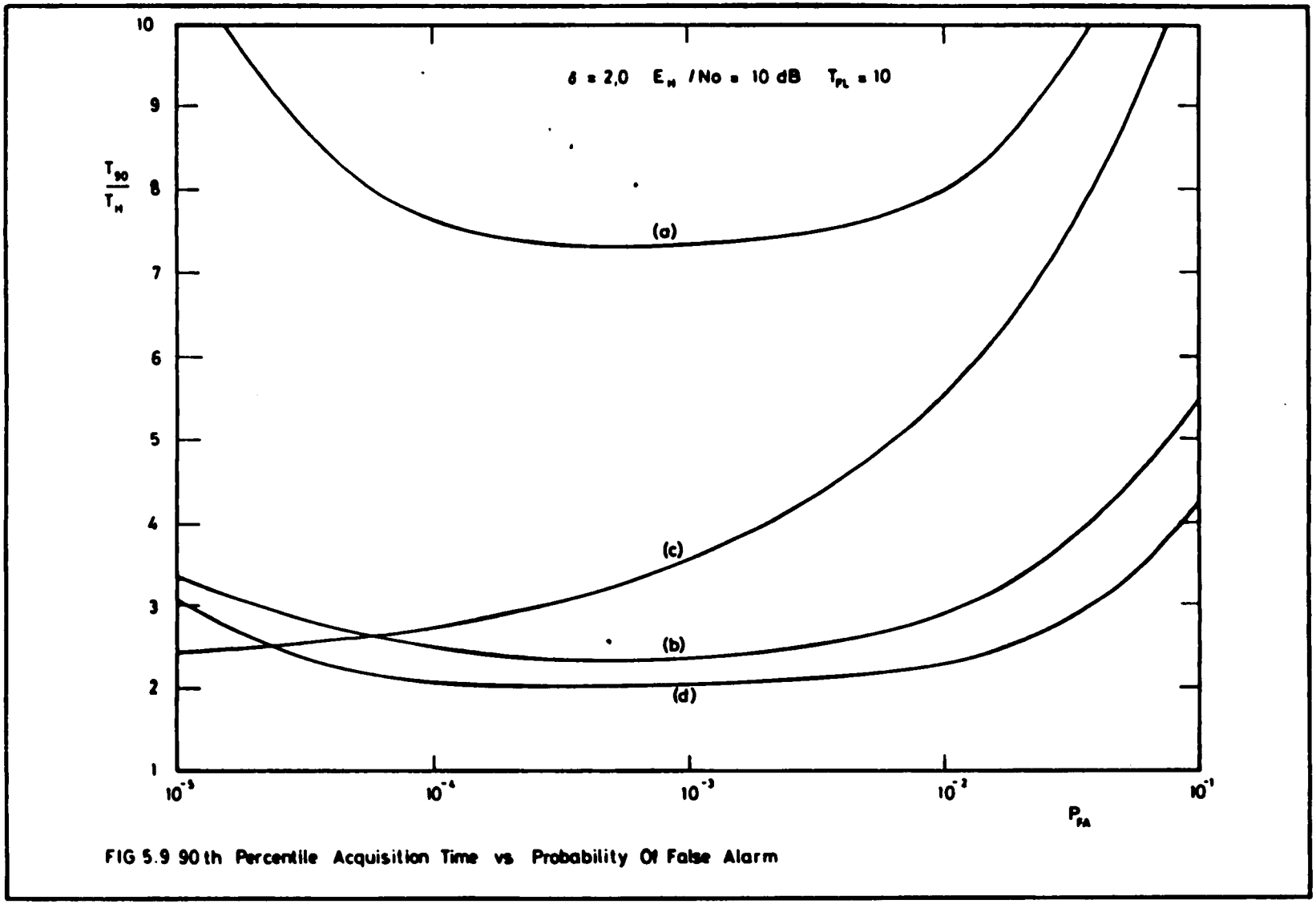

FIG 5.9 90 th Percentile Acquisition Time vs Probability Of False Alarm

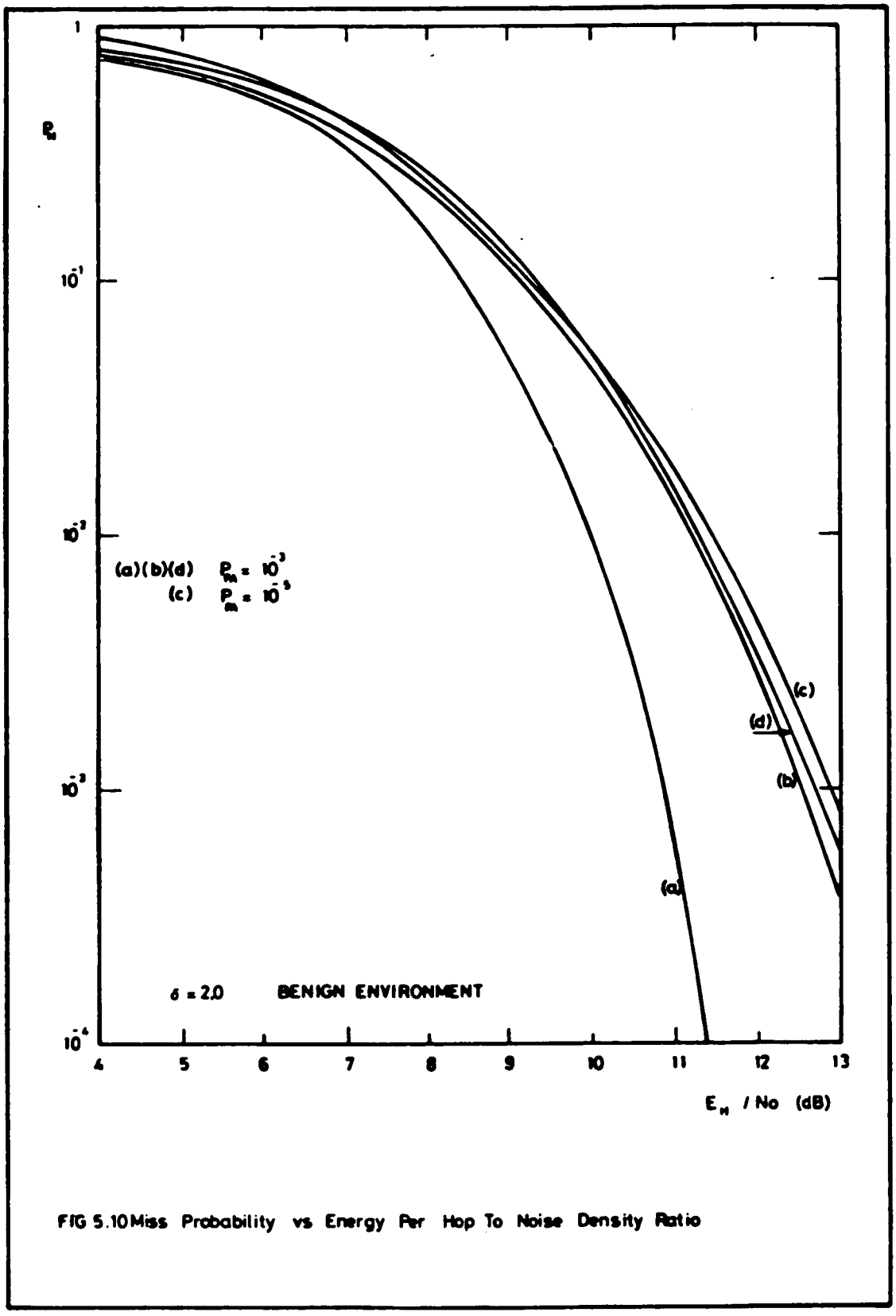

FIG 5.10 Miss Probability vs Energy Per Hop To Noise Density Ratio

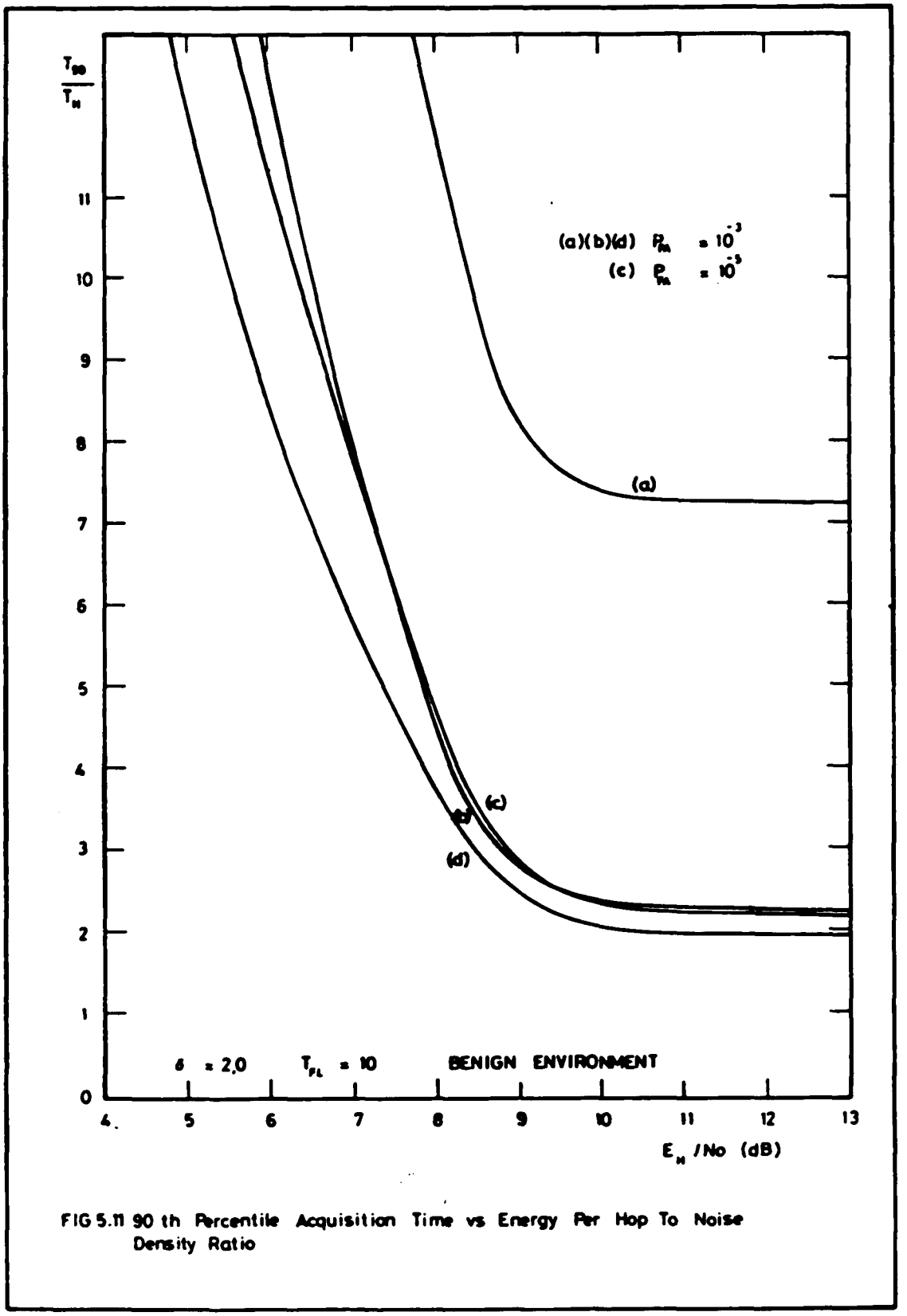

FIG 5.11 90 th Percentile Acquisition Time vs Energy Per Hop To Noise Density Ratio

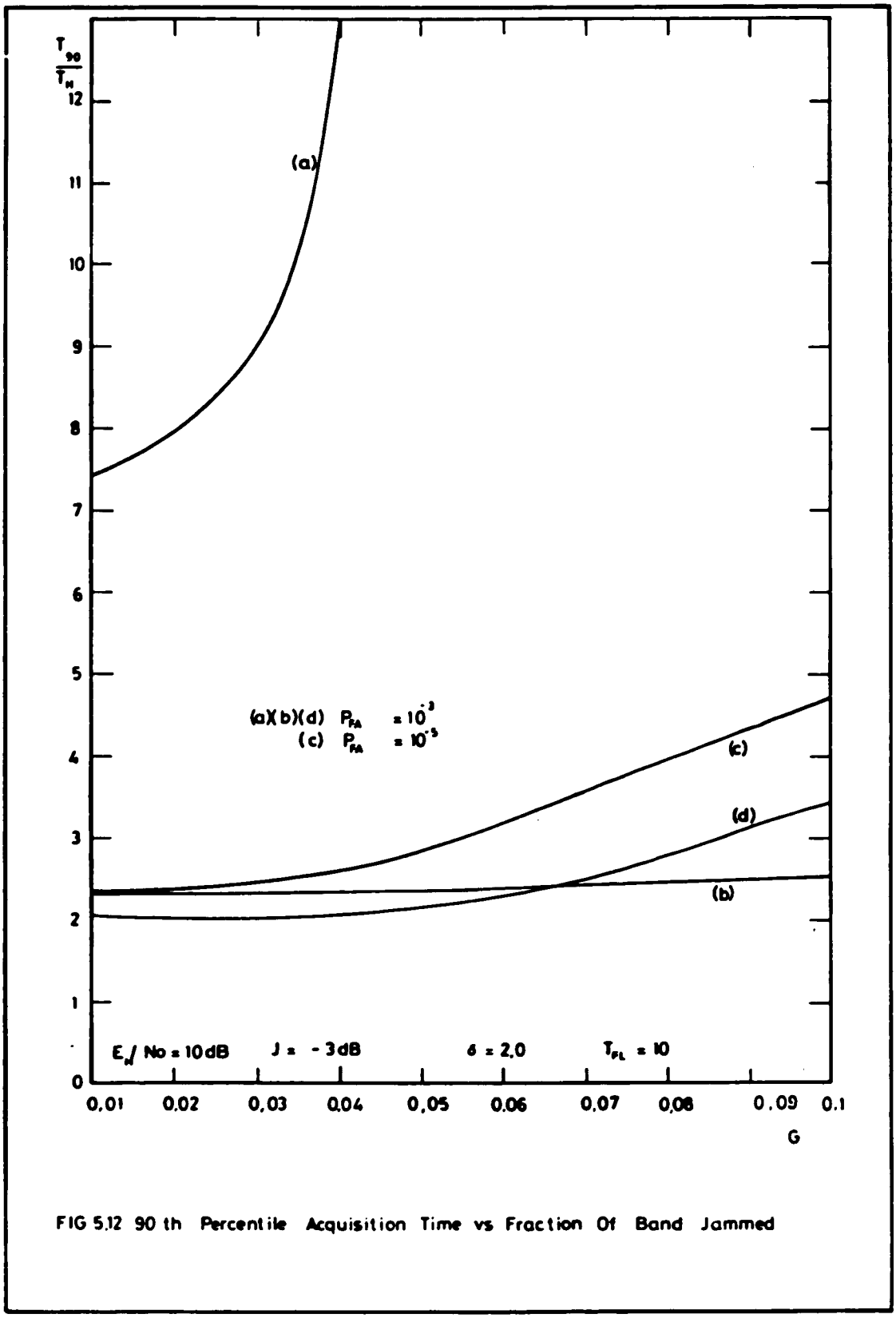

FIG 5.12 90 th Percentile Acquisition Time vs Fraction Of Band Jammed

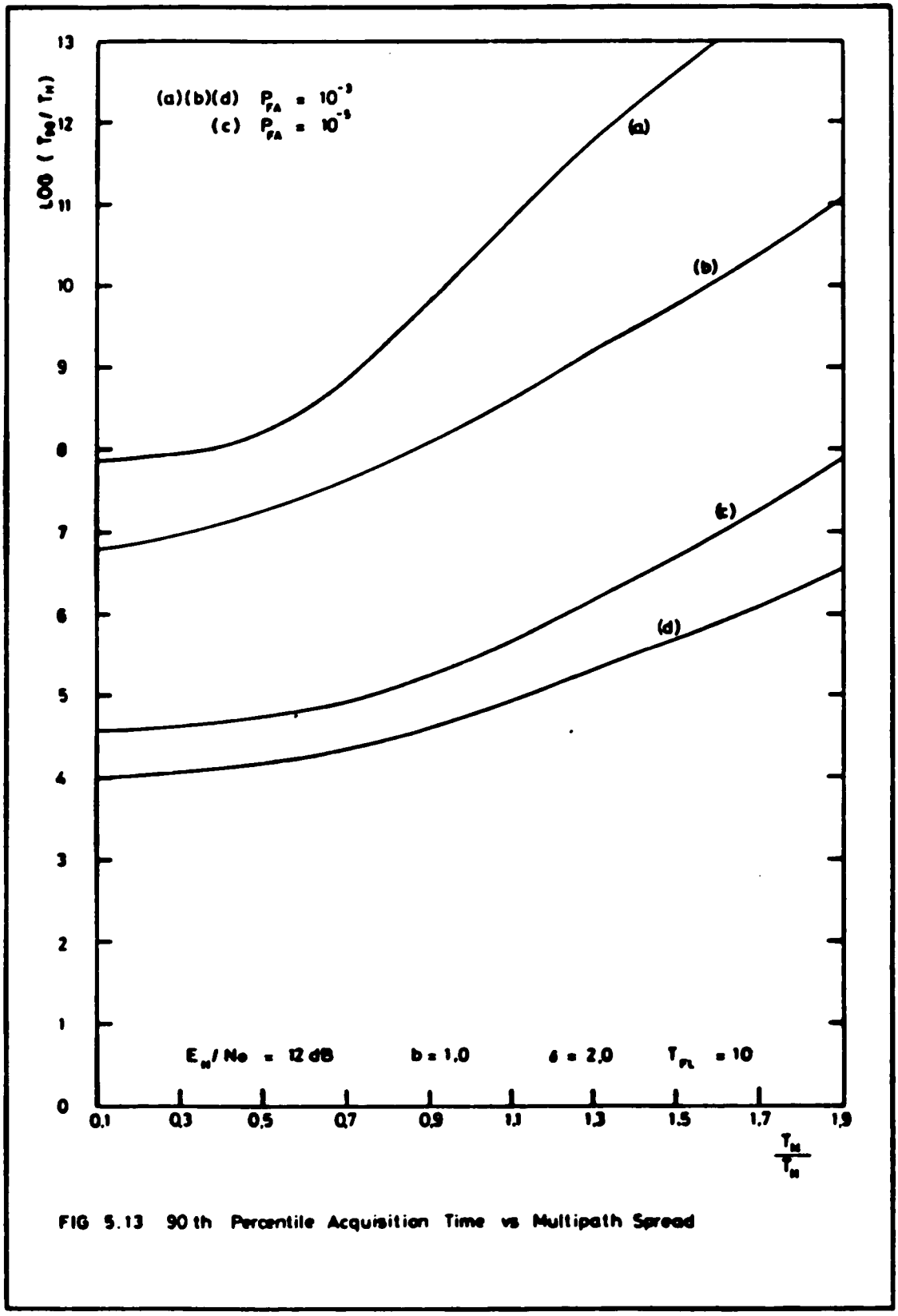

FIG 5.13 90 th Percentile Acquisition Time vs Multipath Spread

a) SIMPLE STRATEGY (n=0) M = 8

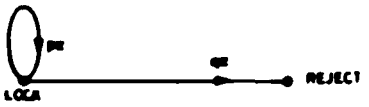

b) SINGLE STAGE STRATEGY (n=1) M = 4

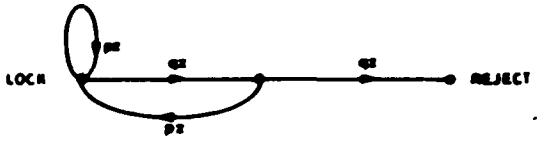

c) CONSECUTIVE COUNT STRATEGY (n=3) M = 2

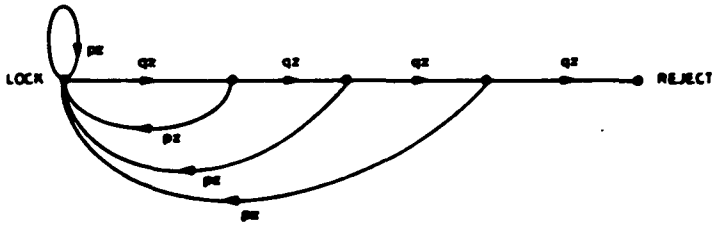

FIG. 5.14 Example Strategies For Tracking

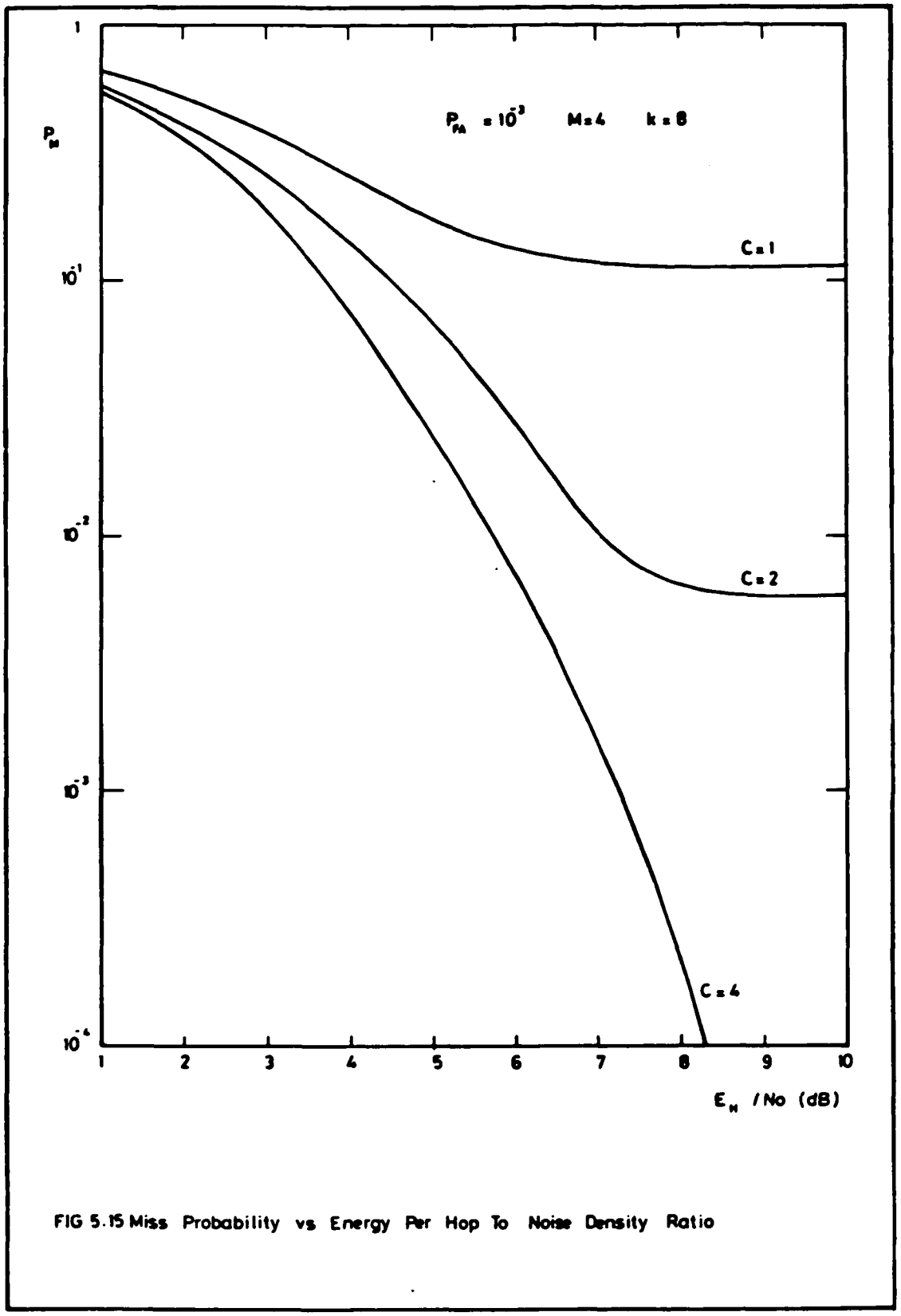

FIG 5.15 Miss Probability vs Energy Per Hop To Noise Density Ratio

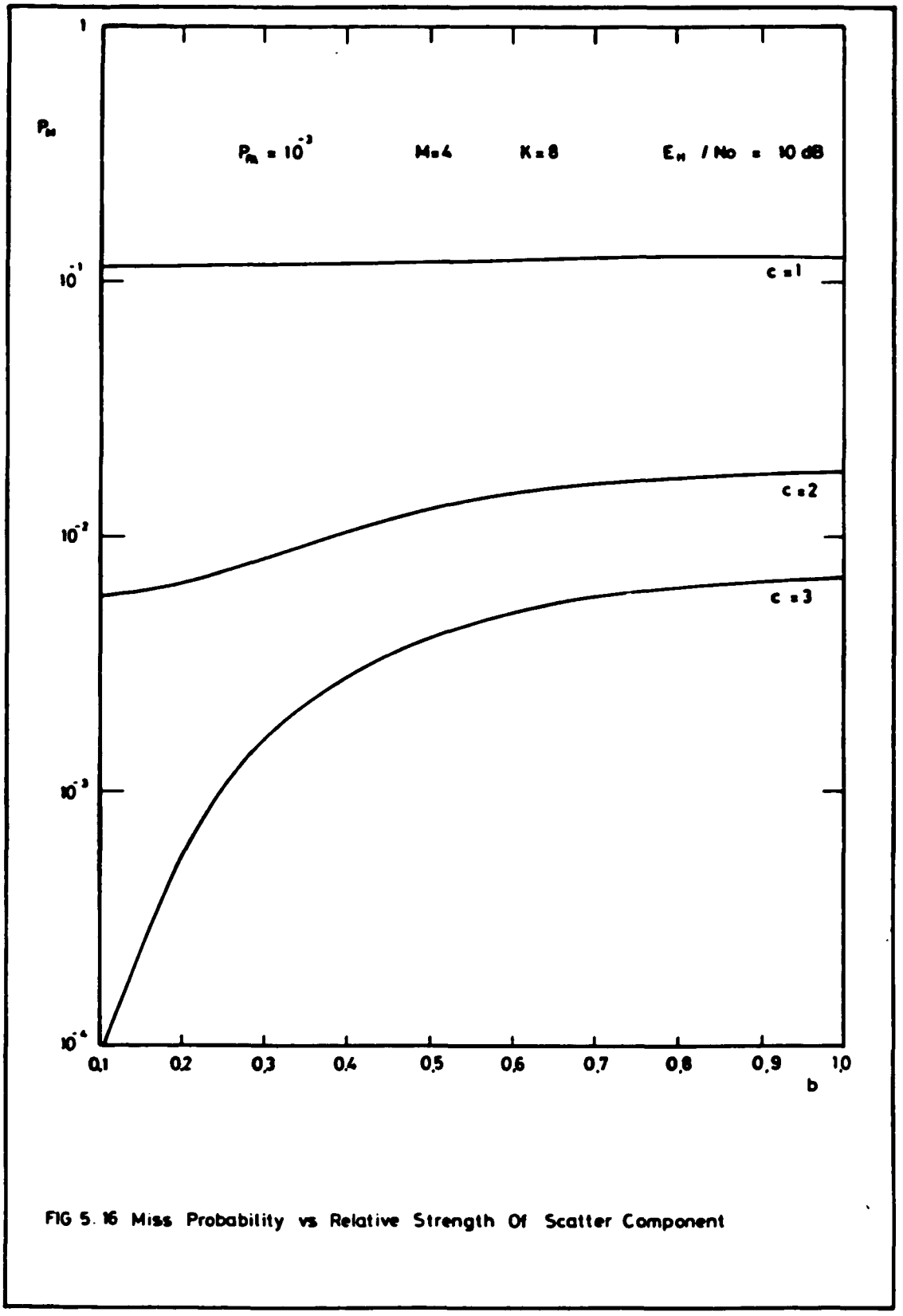

FIG 5.16 Miss Probability vs Relative Strength Of Scatter Component

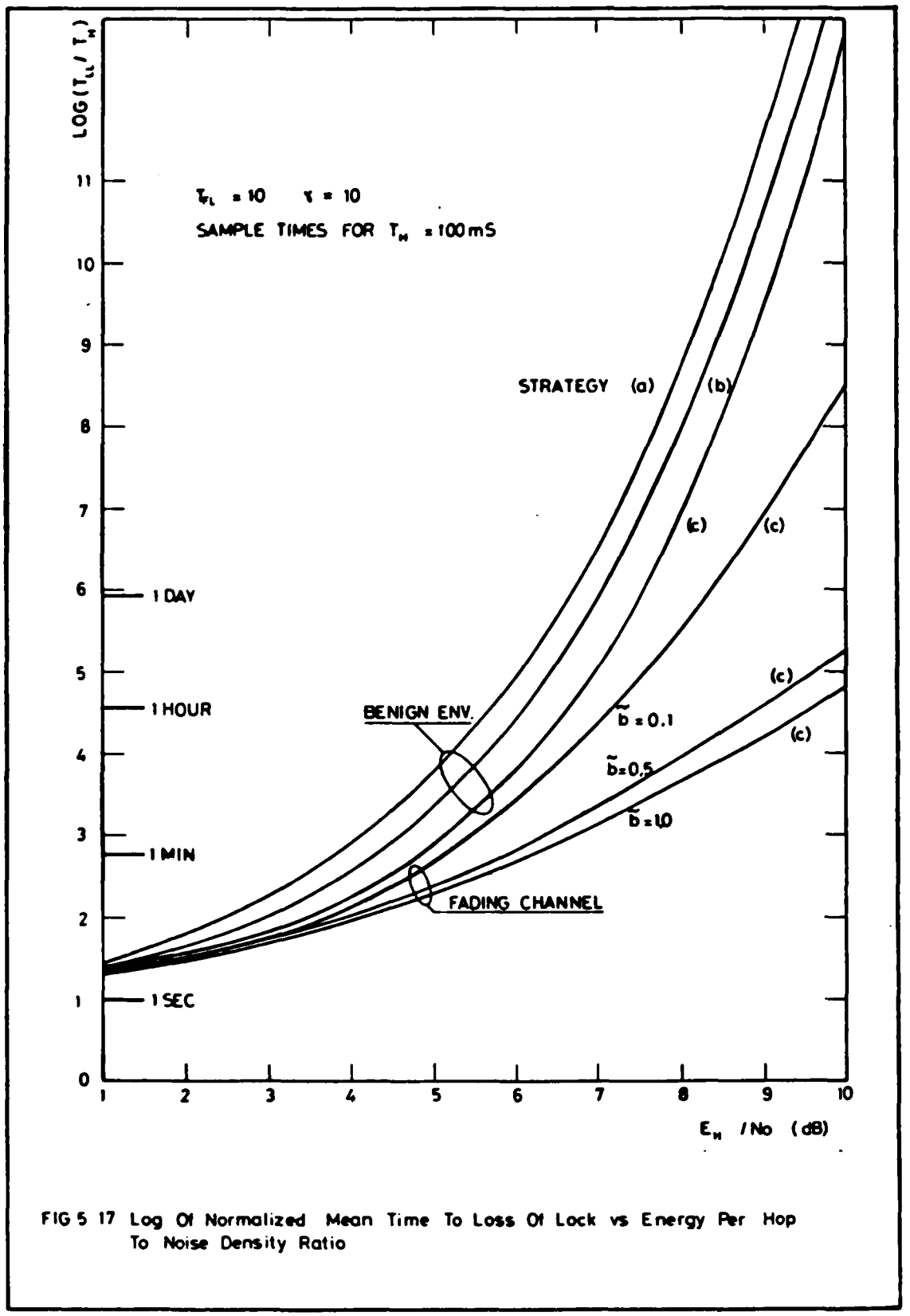

FIG 5 17 Log Of Normalized Mean Time To Loss Of Lock vs Energy Per Hop To Noise Density Ratio

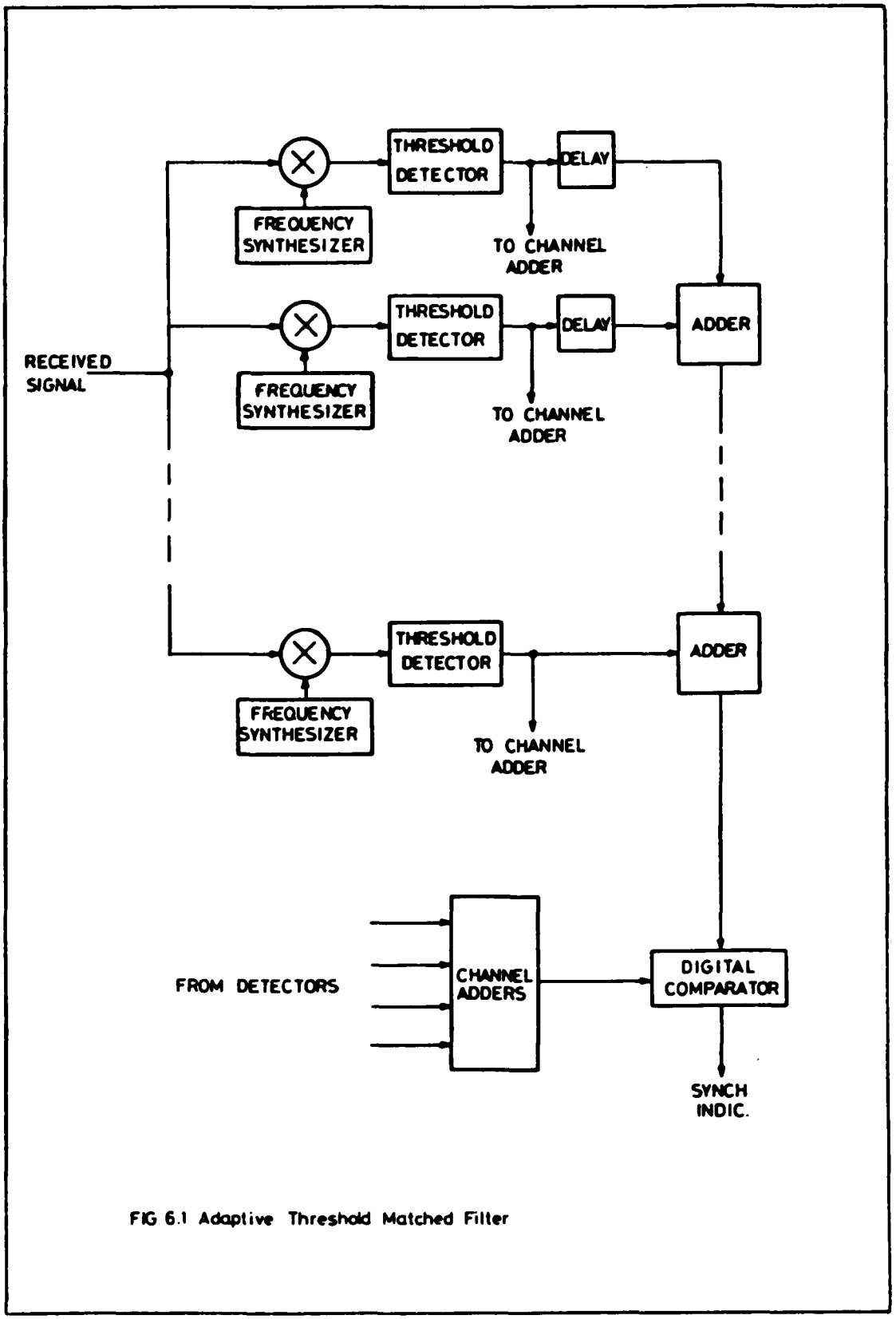

FIG 6.1 Adaptive Threshold Matched Filter

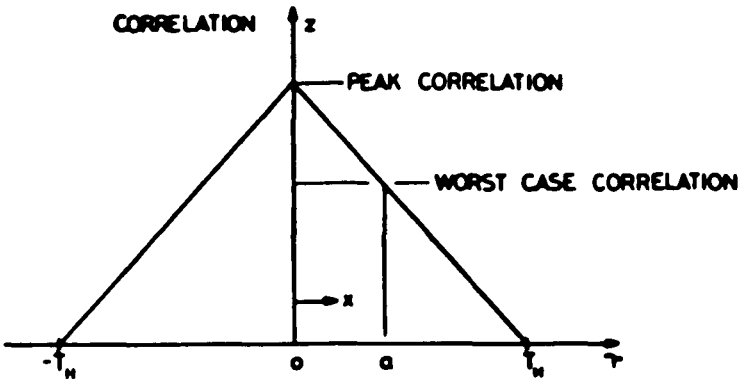

FIG. C1. Correlation Diagram

δ	d	ENERGY LOSS (dB)
1.5	0.875	0.58
2.0	0.75	1.25
0.75	0.75	1.25
0.5	0.5	3.01

FIG. C2. Degradation Factors